Politecnico di Torino

Master Degree in Energy and Nuclear Engineering

Master Thesis

Kinetic modelling of fluidized bed biomass gasification integrated with steam electrolysis for synthetic methane production

Supervisors
Prof. Massimo Santarelli
Ing. Emanuele Giglio

Candidate
Antonio De Padova

October 2021

Abstract

A process configuration for the production of synthetic natural gas (SNG) starting from woody biomass is proposed and analyzed.

A kinetic rate model was developed to simulate the gasification of biomass in a bubbling fluidized bed (BFB) gasifier with a mixture of oxygen and steam as gasifying agent. The model has been then validated comparing its predictions with the experimental results reported in the literature and with the predictions of another model, used as a reference.

The gasification stage performance, in terms of outlet stream composition and temperature, have been then analyzed by varying some parameters like equivalence ratio (ER) and steam-to-biomass ratio (SBR). Proper values of ER and SBR have been set to maximize hydrogen content within the produced syngas.

A solid oxide electrolysis cell (SOEC) system for water splitting has been then modeled. Hydrogen produce at cathode side is mixed with the syngas exiting the gasification unit, to reach the stoichiometric syngas composition for the subsequent methanation reaction, where carbon monoxide and carbon dioxide are hydrogenated in a catalytic reactor to produce synthetic methane. Oxygen-steam mixture from anode outlet is exploited as gasifying agent within biomass gasification unit.

A simple approach for the syngas cleaning was used to take into account all the downstream equipment used to reduce the contaminants (e.g., tars, ammonia, hydrogen sulfide and hydrogen chloride) content in the raw syngas before the methanation unit.

The whole process has been modeled and analyzed using ASPEN Plus process simulator integrated with an external Fortran subroutine to represent properly the gasification stage in terms of hydrodynamics and reaction kinetics.

Acknowledgements

I take this opportunity to express my gratitude to my supervisors, Prof. Massimo Santarelli, for the chance of developing this thesis, and Ing. Emanuele Giglio, for his guidance, patience and availability in any moment during these months.

I wish to express my gratitude to my parents for their constant encouragement and unconditional love.
Thanks to my family and my friends for their support and their presence both in the hard moments and in the joyful ones.
Without all of you I would not be who I am today.

"Happiness is only real when shared."

Contents

List of Figures

List of Tables

Nomenclature

Symbol	Definition
Δh^0	Standard enthalpy of formation [kJ/mol]
$\dot{n}$	Molar flow rate [kmol/s]
ΔG	Change in Gibbs free energy [J]
ΔH	Overall energy demand of reaction [J]
ΔQ	Heat of reaction [J]
T	Temperature [°C] or [K]
ΔS	Entropy variation [J/K]
U	Potential [V]
z	Number of electrones
F	Faraday constant
η	Overvoltage [V]
j	Current density [A/m^2]
S	Active surface area [m^2]
n_C	Number of cells
η_F	Faraday efficiency
$\dot{V}$	Volumetric flow rate [Nm^3/h]
P_{el}	Electrical power [W]
E_S	Specific energy consumption [kWh]
$\dot{m}$	Mass flow rate [kg/s]
d	Diameter [m]
ρ	Density [kg/m^3]
Ar	Archimedes number
g	Gravitational acceleration [m/s^2]
μ	Gas viscosity [Pa· s]
u_{mf}	Minimum fluidization velocity [m/s]
ε_{mf}	Voidage in the emulsion phase [-]
d_{b0}	Initial bubble diameter [m]
N_D	Number of orifices of the distributor plate
A_t	Cross-sectional area of the fluidized bed [cm^2]

u_0	Superficial gas velocity [m/s]
u_b	Bubble rise velocity [m/s]
δ_b	Fraction of bed occupied by bubbles [-]
$vbed_{ave}$	Average bed voidage [-]
ε_f	Volume occupied by the emulsion phase
h_{inc}	Incremental height [m]
C	Molar concentration [kmol/m^3]
p	Pressure [Pa]
R_{gas}	Ideal gas constant [kJ/(kmol · K)]
X	Carbon conversion factor
y_i	Molar fraction of the i-th species
h	Specific mass enthalpy [kJ/kg]

Abbreviation	**Definition**
SOEC	Solid Oxide Electrolytic Cell
SNG	Synthetic Natural Gas
BFB	Bubbling Fluidized Bed
ER	Equivalence Ratio
SBR	Steam-to-Biomass Ratio
DME	Dimethyl ether
NG	Natural Gas
RMSE	Round Mean Square Error
UNFCCC	United Nations Framework Conventions on Climate Change
MOIST	Moisture
ULT	Ultimate Analysis
PROX	Proximate Analysis
RR	Reactant Ratio
RU	Reactant Utilization
OCV	Open Circuit Voltage
ASR	Area Specific Resistance
HHV	Higher Heating Value
LHV	Lower Heating Value
YSZ	Yttrium Stabilized Zirconia
LSM	Lanthanum Strontium Manganite
FEED	Feed Gas Module
FACT	Correction factor used to refer to dry biomass mass flow
WGS	Water Gas Shift
RWGS	Reverse Water Gas Shift
SMR	Steam Methane Reforming

Chapter 1

Introduction

From 1971 to 2018, the World Total Energy Supply (TES) grown very fast: from 5,519 Mtoe to 14,282 Mtoe, it became almost three times bigger (Figure 1.1) [1]. However, in this scenario, conventional fossil fuels still play a dominant role in the energy mix. Due to a decreasing availability of the fossil fuels and to a rising attention to themes like climate change, the renewable energy sources are starting to play a key-role. Their contribution to the energy mix is around the 11%, considering the sum of biofuels and other renewable energy sources.

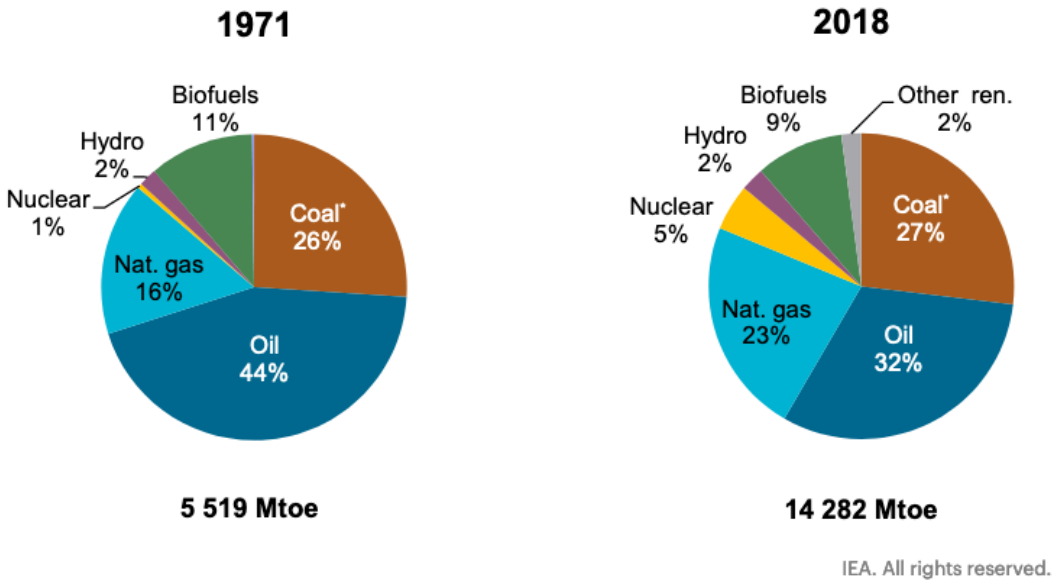

Figure 1.1: Total Energy Supply (TES) by source in 1971 and 2018 [1]

Biomass is for sure one of the most important renewable energy sources, due to its high availability almost everywhere on the Planet. It is also a CO_2

neutral resource: burning fossil fuels converts “old” biomass into “new” CO_2, which is injected in the environment contributing to the “greenhouse effect”, while biomass combustion produces the same CO_2 that it absorbed during its life cycle. Furthermore, biomass does not take millions of years to grow and to develop again, as it happens for carbon or oil, and this is the reason why it is considered a renewable resource [2, 3].

Biomass is exploited with different thermo-chemical processes, mainly combustion, pyrolysis and gasification. With gasification, biomass molecules are broken down to produce gaseous products, named syngas. Syngas can be directly used with energetic purposes or used for the production of secondary products of interest, named biofuels, like dimethyl ether (DME), Fischer-Tropsch products, methanol and synthetic natural gas (SNG). Generally bio-fuels can be used with a series of advantages with respect to the biomass considered as solid fuel. The combustion of a bio-fuel can be better controlled than the combustion of biomass itself, both in terms of operating temperatures and of combustion products. With gasification, and with the following clean-up of its products, it is possible to reduce or to remove the content of polluttants and contaminants like N_2, Cl and S compounds, for example. Additionally, storage and transportation of bio-fuels are definitely more advantageous from a logistic point of view [4].

Natural gas (NG) is one of the major primary fuels and its importance is increasing year by year, replacing coal and oil in many applications (industrial, residential, but also as fuel for vehicles), and playing a key role in the so-called energy-transition.

In this context, the production of SNG supplies a product of great interest which can be injected in the existing distribution grid and can be used for many different purposes [5].

1.1 Research objective

Purpose of this work is to model a plant based on the integration of a gasifier and of a Solid Oxide Electrolytic Cell (SOEC) for the conversion of woody biomass in synthetic natural gas. The integration of these systems for the conversion of biomass in other chemical products of interest has already been treated by several authors: Pozzo et al. for the prodiction of Dimethyl Ether (DME) [6], Bernical et al. for the production of Fischer-Tropsch products [7], Clausen et al. for the production of methanol [8].

Finally, Giglio et al. studied the integration between biomass gasification and high-temperature electrolysis for synthetic methane production, which is

the matter treated in this work too [9].

With respect to this last work, a different approach was used to model the gasification stage: a kinetic rate model was preferred to the thermodynamic equilibrium one.

A 1D model was realized, which is strictly geometry-dependent and gives a better accuracy in terms of composition of the outlet gas stream from the gasification stage.

The proposed model was validated with respect to the experimental results reported by Campoy et al. [10] and its predictions were compared to the ones reported by Dang et al. [11], showing a good overall accuracy in terms of Round Mean Square Error (RMSE). In this first phase of model validation, a mixture of steam and air was considered as gasifying agent.

Then the reactor geometry was adapted, considering as gasifying agent a mixture of steam and pure oxygen. With respect to the previous validation phase, the input gas superficial velocity was kept constant, leading to a reduction of the geometry of the gasifier.

Subsequently a SOEC was modeled with two main goals: to supply the gasifying agent (oxygen and steam) to the gasifier and, mainly, to enrich the H_2 content of the syngas produced, to ensure the respect of the stoichiometric requirement for the subsequent methanation reaction. The modeling of this integrated system was performed using APEN Plus software. In particular the gasification stage was modeled with a User defined block “User2”, linked with an external FORTRAN subroutine, used to represent bed hydrodynamics and reaction kinetics. This is the main difference with respect to the previous 0D equilibrium model.

Among all the different types of biofuels which can be produced by the integration of the gasifier and the electrolytic cell, SNG was chosen because methanation reactions are highly exothermic, more than the synthesis reactions of other biofuels (for example methanol):

- *Methane synthesis reactions*
  $CO + 3H_2 \rightarrow CH_4 + H_2O \qquad \Delta h^0 = -206\ kJ/mol$
  $CO_2 + 4H_2 \rightarrow CH_4 + 2H_2O \qquad \Delta h^0 = -165\ kJ/mol$

- *Methanol synthesis reactions*
  $CO + 2H_2 \rightarrow CH_3OH \qquad \Delta h^0 = -91\ kJ/mol$
  $CO_2 + 3H_2 \rightarrow CH_3OH + H_2O \qquad \Delta h^0 = -50\ kJ/mol$

This is an interesting aspect since the generated heat can be exploited for a thermal integration. About the electrolyzer, the SOEC was chosen for this investigation since it ensures high efficiencies associated with lower costs for hydrogen production [12]. Nevertheless it is not widely used as technology yet, mainly due to some structural problems and materials degradation that can occur due to its high operating temperatures (in the range of 700-900°C usually).

Chapter 2

Technology review

2.1 Biomass

It is hard to find a unique definition of biomass. The United Nations Framework Conventions on Climate Change (UNFCCC) defined it as:

A non fossilized and biodegradable organic material originating from plants, animals and micro-organisms. This shall also include all products, residues and wastes from agriculture, forestry and related industries as well as the non-fossilized and biodegradable organic fractions of industrial and municipal wastes [13].

Unlike fossil fuels, biomass does not take millions of years to grow and develop. For this reason, it is considered one of the most important renewable energy sources.

It can also be considered a "carbon neutral" resource, since its deployment does not add "new" CO_2 to the environment. Plants use solar energy to combine carbon dioxide and water, converting them into carbohydrates $(CH_2O)_n$ and oxygen in presence of sunlight, clorophyll and water, in a process called photosynthesis. The sugar formed is stored in a polymer form as cellulose or hemicellulose [14].

$$nCO_2 + nH_2O + light \rightarrow (CH_2O)_n + nO_2$$

2.1.1 Biomass composition

The biomass main constituents are lignocellulose - which is mainly made up by cellulose, hemicellulose and lignin - and a large number of complex organic compounds. Furthermore, there is an important amount of water stored in form of moisture $(MOIST)$ and a small amount of inorganic impurities, known as ash (ASH).

The principal constituting elements are carbon (C), hydrogen (H), oxygen (O), nitrogen (N), chlorine (Cl) and sulphur (S), even if these last three are usually present in very small amounts.

It is very important to know the feedstock composition, in order to determine its potential to produce a valuable product.

The feedstock composition can be given in terms of ultimate and proximate analysis.

- **Ultimate analysis**
  Composition expressed in terms of basic elements, moisture and ash content. It is expressed as weight percentage of the constituent elements, usually on a dry basis. So we can find it expressed as:

  $$C + H + O + N + S + Cl + ASH = 100\%$$

  The larger the amount of carbon and oxygen in the feedstock, the greater the amount of CO and CO_2 that will be produced during gasification. At relatively low temperatures, CH_4 is produced too, but its content will decrease with increasing temperature, while CO_2 and CO content will increase due to the methane reforming and decomposition reactions [15].

- **Proximate analysis**
  It gives the composition in terms of gross components, such as moisture $(MOSIT)$, Volatile Matter (VM), ash (ASH) and Fixed Carbon (FC). The volatile matter is the condensable and noncondensable gaseous phase released when the fuel is heated. Its amount depends on some operating parameters, like temperature or the process heating rate.

  Ash is the inorganic solid residue left when the fuel is completely burned. It is mainly constituted by silica, aluminium, calcium and other minerals. They lead to some problems for the reactor, such as plugging and sintering of the catalysts, especially at high temperatures.

Fixed Carbon (FC) represents the solid carbon in the biomass that remains in solid phase after the devolatilization (char).

2.1.2 Biomass conversion

The conversion of solid biomass into secondary products, like liquid and gaseous biomass-derived fuels, can be achieved mainly through two pathways: biochemical conversion (fermentation) and thermochemical conversion (pyrolysis, gasification).

In this work we will focus on the second pathway, and in particular on the gasification process.

There are several reasons to convert biomass into secondary products [16]:

- secondary products are more energy dense and can be handled more easily: unlike gases or liquids, in fact, solid biomass has great dimensions, which makes difficult to store or to transport it;
- the producer gas from a gasifier can be used in a wider range of applications than a solid fuel. It can produce valuable chemicals as side products (methanol, gasoline, fertilizers, etc.);
- flue gases obtained from gasification is less than those obtained from a direct combustion system;
- if the gas obtained from gasification will be used for energy purposes, like combustion in internal combustion engines, SO_X and NO_X emissions are lower, since the syngas is cleaned from its contaminants before being used.

On the other hand, if heat is the only desired product, combustion is preferable and more economical.

2.2 External drying

Woody biomass has a high water content, which could also be up to 50% wt. on a wet basis. The moisture content depends on several parameters, like the wood type, the harvesting season and the storage locations and conditions, in terms of temperature, humidity of the air, etc.

The external drying of biomass is a very important preliminary stage. Its aim is to reduce the moisture content of the raw biomass before feeding it

to the gasifier or, in general, to the thermochemical process of interest. The biomass water content, in fact, has a great impact on gasification performances and efficiencies, as it absorbs heat to be evaporated, and that is the main reason why it should be as low as possible [17].

On the other hand, the drying operation has a large impact on the energy balance of the plant overall [18].

The water content is decreased first with a natural drying process, which occurs during the storage period. The speed of this natural process depends on the storage system, in terms of place and duration, the air temperature and the starting water content itself in the stored raw biomass. Usually it is possible to reduce the moisture content up to a value of 30%. If the biomass is stored for too much time – which means over six months – a fraction of organic matter is lost too, due to the natural degradation that occurs. Biomass can lose up to 10-30$\%$ of its organic matter per year in this way [17].

To reach values lower than the 30% of moisture left, it is necessary to use industrial dryers, at least to accelerate the process and to avoid the loss of organic matter.

Several technologies are available for the forced biomass drying and they differ one from another depending on some parameters and on the available heat sources. The heat sources of the dryer can be hot flue gases or steam. The drying medium can operate in a closed loop with a purge to evacuate humidity or can be a once through air stream. Usually, ambient air is heated to lower its humidity and to activate the drying kinetics.

The efficiency of the drying process is less than 50% at low temperatures and it increases with the temperature. At temperatures higher than 160°C, biomass starts to release volatile compounds, and this leads to volatile matter losses and to an increase in the cost of the purification of the drying air [17]. For these reasons it is recommended to keep the drying temperature at values lower than 160°C.

2.3 Gasification

Gasification is the thermochemical conversion of carbonaceous feedstock, like biomass in this case, into a synthetic gas, called syngas, mainly made up by hydrogen (H_2) and carbon monoxide (CO), which can be used directly for power generation purposes or for secondary fuels production. Also a residual solid phase, called “char”, is generated, which includes the organic unconverted fraction and the inert material (ashes) present in the biomass [19].

There are three main reasons to chose gasification as thermochemical conversion process for biomass:

1. It is possible to increase the produced gas quality, removing non-combustible gases such as nitrogen or water. This increases the heating value of the produced gas;

2. It is possible to reduce the air pollution, removing sulphur and nitrogen compounds from the produced gas before it is used in combustion engines, for example;

3. It is possible to increase the relative hydrogen content of the fuel.

Gasification needs a so-called “gasifying agent” to occur, which is usually air, oxygen, steam or a mixture of them. In general, it occurs in a oxygen-deficient environment, and this leads to a partial oxidation of the feedstock.

It is possible to recognize three different stages during a gasification process:

- **Drying and devolatilization (or pyrolysis)**
  It is an endothermic stage. When the biomass is sent to the gasifier, it starts to be heated and releases its moisture content and starts to be decomposed, leading to the formation of lighter molecules. In this stage, three main products are obtained: non-condensable gases - which are mainly CO, CO_2, CH_4, H_2, H_2O and light hydrocarbons -, tars - or liquid fraction, meaning that all these gaseous compounds condense at lower temperatures - and char (Figure 2.1).

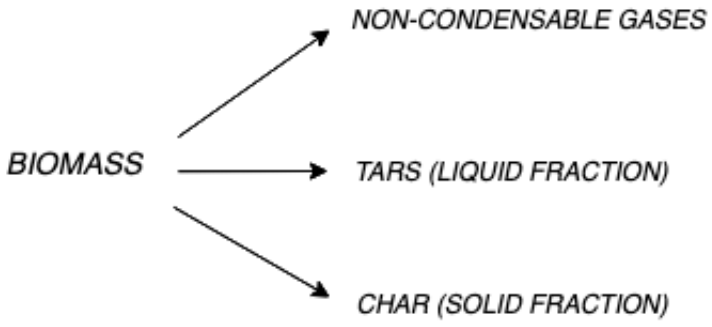

Figure 2.1: Devolatilization products

This step usually takes place at temperature ranging from 250 to 700°C. Devolatilization stage can be represented by the following equation [19]:

$$Biomass \rightarrow CO{+}CO_2{+}H_2{+}CH_4{+}H_2O(g){+}Tars{+}Char \qquad (endothermic)$$

- **Oxidation**
  It is a very important stage since, being exothermic, it provides the necessary heat to all the other endothermic stages which occur during the gasification. This is the reason why gasification can be considered an auto-thermal process and does not require an external heat source. Oxidation is carried out in a oxygen-deficient environment or, in other words, with an amount of oxygen which is much lower than the stoichiometric amount needed for a complete combustion. The main oxidation reactions that occur are:

$C + O_2 \rightarrow CO_2$	$\Delta h^0 = -394\ kJ/mol$	[19]
$C + 0.5O_2 \rightarrow CO$	$\Delta h^0 = -111\ kJ/mol$	[19]
$CO + 0.5O_2 \rightarrow CO_2$	$\Delta h^0 = -283\ kJ/mol$	[19]
$H_2 + 0.5O_2 \rightarrow H_2O$	$\Delta h^0 = -242\ kJ/mol$	[20]
$CH_4 + 1.5O_2 \rightarrow CO + 2H_2O$	$\Delta h^0 = -802{,}31\ kJ/mol$	[20]

- **Reduction**
  It involves all the products of the preceding stages of pyrolysis and oxidation. All the gas species and the char react with each other, both in heterogeneous and homogeneous reactions, generating the final syngas. The main reactions which occur are:

$C + H_2O \rightarrow CO + H_2$	$\Delta h^0 = +131\ kJ/mol$	[20]
$C + CO_2 \rightarrow 2CO$	$\Delta h^0 = +172\ kJ/mol$	[20]
$CO + H_2O \rightarrow H_2 + CO_2$	$\Delta h^0 = -41\ kJ/mol$	[20]
$CH_4 + H_2O \rightarrow CO + 3H_2$	$\Delta h^0 = +206\ kJ/mol$	[20]

The reduction zone temperature has a key role for the determination of the final syngas composition. This because the endothermic reactions are favored at high temperatures, while the exothermic reactions are favored at lower temperatures.

It is important to say that all these stages are not independent and sequential - even if in this work they were modeled in this way - but actually they occur all at the same time.

2.3.1 Types of gasifiers

Several classifications of gasification reactors can be done on the basis of:

- Gasification agent: mainly air-blown gasifiers, oxygen gasifiers, steam gasifiers;
- Heat source: auto-thermal or direct gasifiers, where the heat is supplied by the partial combustion of the biomass, and allothermal or indirect gasifiers, where heat is supplied by an external heat source;
- Gasifier pressure: atmospheric or pressurised gasifiers;
- Reactor design: fixed bed gasifiers, fluidized bed gasifiers, entrained flow gasifiers.

The following paragraphs about the different types of gasifiers are taken and adapted from Basu [16], which is recommended for further and more detailed informations.

2.3.1.1 Fixed bed gasifiers

These are the simplest kind of gasifiers. The fuel is supported on a grate on the bottom of the reactor, which usually is made moving, for example rotating, and that is the reason why these kind of reactors are also called “moving bed reactors”. The fuel moves down in the gasifier from the top. However, due to their configuration, both mixing and heat transfer within the bed are poor, which makes difficult to achieve a uniform distribution of fuel and temperature across the gasifier.
There are three main types of fixed-bed gasifiers:

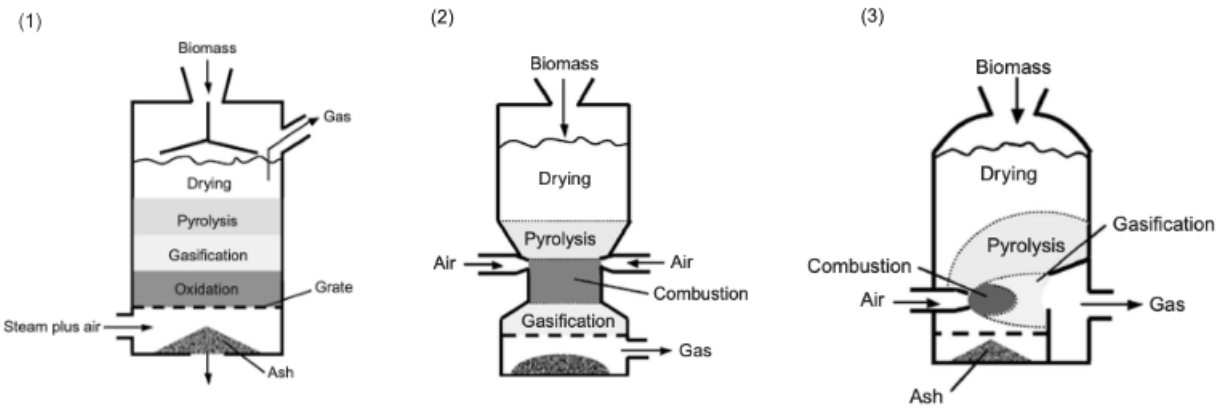

Figure 2.2: Fixed bed gasifiers: 1. updraft gasifier, 2. downdraft gasifier, 3. crossdraft gasifier [16].

- **Updraft gasifier** The gasifying agent enters from the bottom and moves towards the top, while the biomass is loaded from the top and moves downward, so gas and solids are in counter-current mode. The product gas leaves from near the top of the gasifier. Entering the reactor, the gasifying agent passes through the grate, where it meets the combustion zone, with a very high temperature. The hot gas with its low oxygen content moves upward transporting heat to the other zones of the gasifier. As biomass enters from the top, it experiences drying, devolatilization and gasification, then oxidation. The syngas temperature at the outlet is low, so the tar content is quite high, since the gas does not experience the high temperature required for tar cracking (Fig. 2.2.1).
- **Downdraft gasifier** It is a co-current reactor, where the gasifying agent enters the gasifier at a certain height below the top. The product gas flows downward, and leaves from lower section of the gasifier through a bed of hot ash. Since it passes through the high-temperature zone of hot ash, the tar in the product gas finds favorable conditions for cracking reactions, so the tar content is very low. An important requirement for this kind of reactor is that the biomass must have a low moisture content, since biomass first meets “low temperature” gases, so it has not heat enough available to be dried, as it happens for example in the updraft gasifier (Fig. 2.2.2).
- **Crossdraft gasifier** It is a co-current moving bed reactor, in which the fuel is fed from the top while the gasifying agent is injected through a

nozzle from the side of the gasifier. The produced gas is released from the sidewall opposite to the entry point of the gasifying agent, so the gas is produced in the horizontal direction. This means that there is an high temperature in a relative small volume, leading to a very good char conversion and to a very low tar content for the produced gas. Anyway, this solution is not very used (Fig. 2.2.3).

2.3.1.2 Fluidized bed reactors

A fluidized bed is made of fuel particles of specified size and mixed with granular solids of another material called bed particles, which are kept in a semi-suspended condition (fluidization) by the passage of the gasifying agent through them at appropriate velocities from the bottom.

Fluidized-bed gasifiers' main characteristics are their excellent reactants mixing and temperature uniformity.

A drawback of these reactors is that they usually produce a gas with high particulate content, represented both by the bed material and the solid residual produced from biomass, so a downstream cyclone is necessary as part of the installation.

The fluidized bed design has proved to be particularly advantageous for the gasification of biomass. The gas outlet temperature is usually quite high (about 900°C), so its tar production has been found to be between that for updraft (about 50 g/Nm^3) and downdraft gasifiers (about 1 g/Nm^3), with a typical value of 10 g/Nm^3 [21].

- **Bubbling fluidized bed gasifier**
  It was first developed by Fritz Winkler in 1921. It can operate both at low or high temperatures and at atmospheric or elevated pressures. The bed materials are fluidized with steam, air, oxygen or their combination, depending on the choice.

  Two phases can be recognized in a bubbling bed gasifier: a dense phase, with an high solid content, located at the bottom of the reactor, and a diluted phase, called freeboard.

  In the lower zone gas bubbles formation and implosion generate high turbulence, favouring mixing of the solid components.

  The fluidization velocity has to be higher than a certain value called minimum fluidization velocity, which is the velocity which ensures the fluidization of the bed materials. Typical values of fluidization velocities for BFB reactor are around 1 m/s (Figure 2.3.1).

- **Circulating fluidized bed gasifier** With respect to BFB gasifiers, it has higher values of superficial gas velocity, usually in the range 3.5-5.5 m/s.

  Due to the higher velocities, the solids are dispersed all over the tall riser, allowing a long residence time for the gas and for the fine particles, and this ensures a good carbon conversion.

  It is also designed to operate under pressurized conditions in order to increase the final products' yield (Figure 2.3.2).

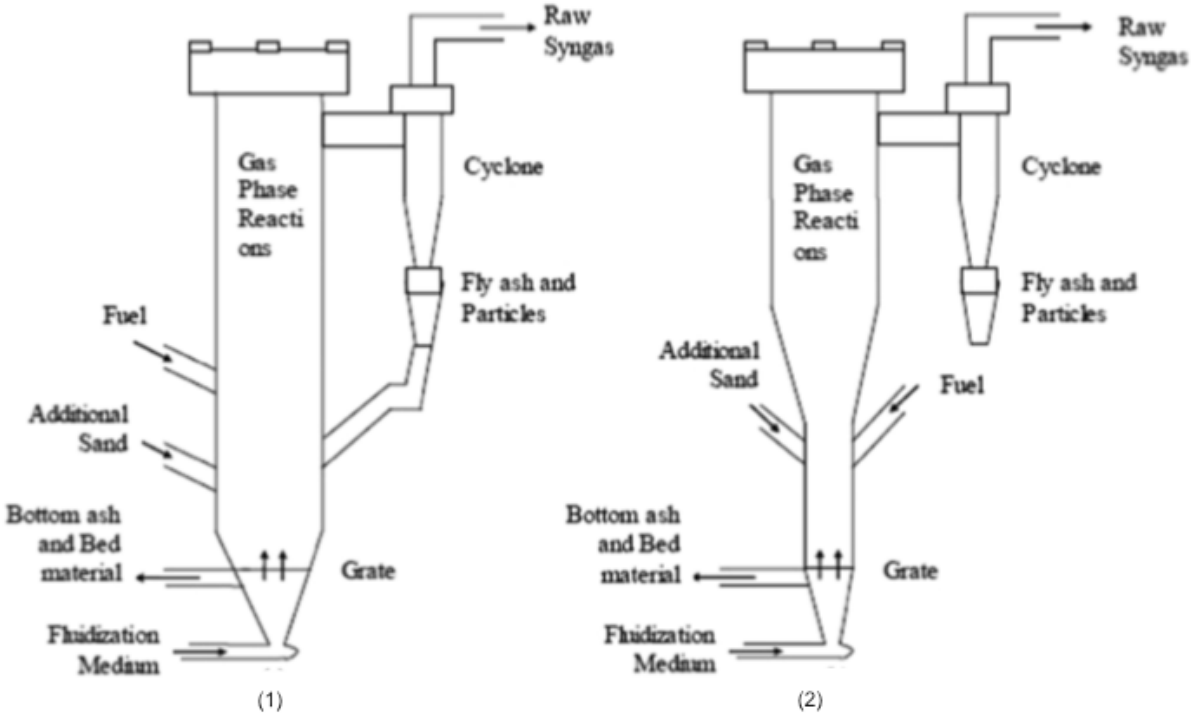

Figure 2.3: Fluidized bed gasifiers: 1. Bubbling fluidized bed gasifier, 2. Circulating fluidized bed gasifier [22].

2.3.1.3 Entrained flow gasifiers

Fine particles and gasifying agent are fed co-currently from the top of the reactor. This results in the gas surrounding or entraining the solid particles as they flow through the gasifier in a dense cloud.

They operate at high temperatures (1300-1500°C) and pressures (25-30 bar) and they are characterized by an extremely turbulent flow which causes rapid and efficient carbon particles conversion (near to 100%).

In general, this solution is preferred more for coal than for biomass, since it is very difficult to grind biomass into such fine dimensions required by this kind of reactor, due to the biomass' high moisture content.

The high gasification temperatures allow to have a product gas which is nearly tar-free and has a very low methane content.

Furthermore, in entrained flow gasifiers ashes are molten, due to the quite high temperatures which are reached. Molten biomass ash is highly aggressive and this reduces the gasifier's life.

A typical entrained flow gasifier simplified scheme is reported in Figure 2.4.

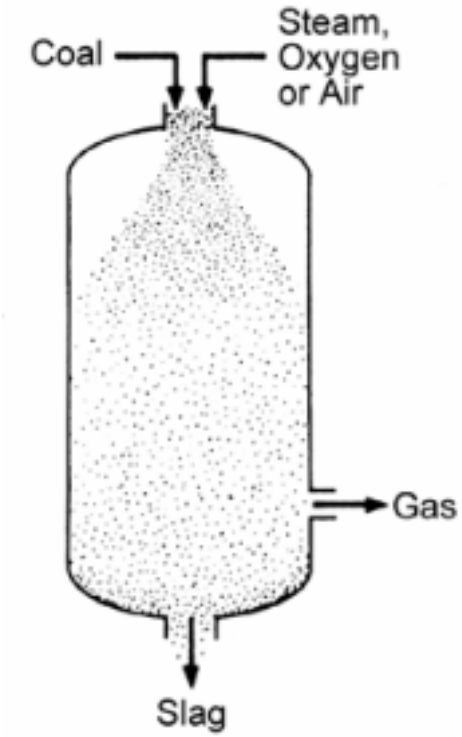

Figure 2.4: Entrained bed gasifier [23]

2.3.2 Equivalence Ratio (ER) and Steam-to-Biomass Ratio (SBR)

Equivalence ratio (ER) and Steam-to-Biomass Ratio (SBR) are two important parameters to define gasifier operating conditions in terms of gasifying agent flow sent to the gasifier.

Equivalence ratio (ER) is defined as the ratio between the mass flow of oxygen supplied as gasifying agent and the theoretical mass flow of oxygen required for the stoichiometric combustion of the biomass.

$$Equivalence\ Ratio\ (ER) = \frac{O_2\ mass\ flow\ fed\ to\ the\ gasifier}{O_2\ mass\ flow\ required\ for\ stoichiometric\ combustion}$$

As it will be seen later, increasing the mass flow of gasifying oxygen – so ER – leads to an increase of combustion products (CO_2 and H_2O), which means higher temperature and lower syngas yield and heating value.

Typically ER ranges from 0.2 to about 0.4 [24].

In order to set the gasifying-O_2 mass flow to send to the gasifier, it is first needed to know the mass flow of oxygen required for the stoichiometric combustion of that biomass feedstock.

It is known that 1 kg of carbon needs 2.667 kg of oxygen, 1 kg of hydrogen needs 8 kg of oxygen and 1 kg of sulphur requires 1 kg of oxygen to be completely burnt.

Knowing the biomass elemental composition from its ultimate analysis, it is possible to approximate the mass flow of oxygen required for the stoichiometric combustion as:

$$O_{2,stoich} = 2.667 \cdot C + 8 \cdot H + S - O$$

Where C, H, S and O are the mass flows of the corresponding elements in the considered biomass [kg/h].

Steam-to-Biomass Ratio (SBR) is the ratio between the steam mass flow fed to the gasifier and the biomass mass flow fed to the gasifier.

$$Steam\,to\,Biomass\ Ratio\ (SBR) = \frac{Steam\ mass\ flow\ fed\ to\ the\ gasifier}{Biomass\ mass\ flow\ fed\ to\ the\ gasifier}$$

Steam-to-Biomass ratio can be changed by varying biomass mass flow and keeping constant steam mass flow, or vice-versa. Higher SBR values mean both a decrease in the gasification temperature and an increment in the water

content in the produced gas. Also an important energy cost is required to produce more steam, so it is necessary to select an optimal SBR according to different operating conditions.

2.3.3 Tars formation

The term “tar” usually refers to a broad range of organic compounds that are in the form of vapour at the gasification temperature (above 400°C) but liquid at ambient temperature.

Generally, tars are all those organic compounds with molecular weight greater than benzene [25].

They can be classified into primary, secondary and tertiary tars (Figure 2.5).

- **Primary tars** (or wood oil) are released directly during the devolatilization step, and mainly depend on the type of biomass. Typical primary tars, as listed by Milne and Evans [21] may be: alcohols, ketones, aldehydes, phenols, etc.;
- **Secondary tars** can be formed during the oxidation step, as consequence of the increase in temperature that causes the reforming of the primary tars into smaller, lighter non-condensable gases and into a series of heavier molecules. Phenols and olefins are important constituents of this group of tars;
- A further increase of temperature leads to the decomposition (cracking) and recombination of secondary tars into the so called **tertiary (or high-temperature) tars**. Tertiary tars start to appear only when primary tars are completely converted into secondary, so they cannot coexist with primary tars. It is possible to further distinguish between:

  1. Alkyl tertiary product: including methy derivatives of aromatics, toluene and indene.;

  2. Condensed tertiaty aromatics: polynuclear aromatic hydrocarbon (PAH), like benzene, naphtalene, acenaphthylene, etc.

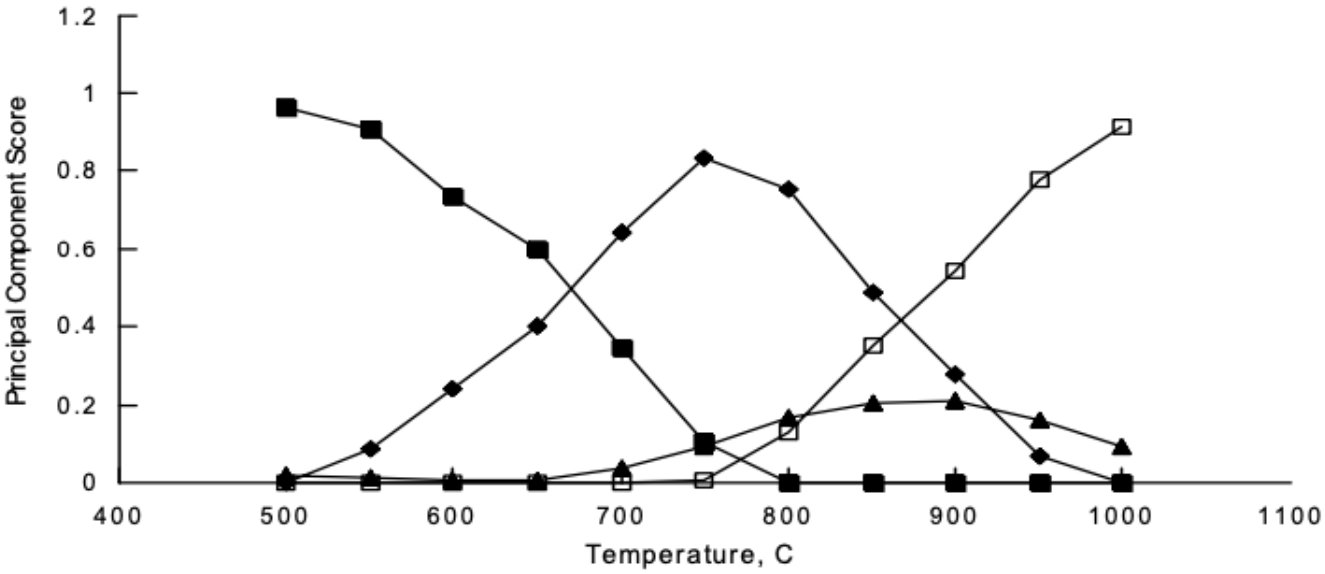

Figure 2.5: Distribution of tar species as a temperature function [21]

In general tar is an highly undesirable product, as it can create many problems to the reactor, including:

- Condensation and subsequent plugging of downstream equipment, where there is a temperature reduction;
- Formation of tar aerosols;
- Polymerization into more complex structures.

Tar in coal gasification comprises benzene, toluene, xylene, etc. and all these compounds have a good commercial value.

Tar from biomass, on the other hand, is mostly oxygenated, due to an higher oxygen content of biomass with respect to coal, and has little commercial use.

The tar content has to be reduced, in order to make the produced gas suitable for gas engines applications - and in general for all the other possible downstream utilisations of the syngas - since their presence would lead to a series of problems for the engine and its equipments, as previously said. So tar removal remains an important part of the development and the design of biomass gasification plants.

2.4 Electrolysis

Water electrolysis is the process which allows to convert water and DC electricity into gaseous hydrogen and oxygen, which is the reverse of what an hydrogen fuel cell does.

In a Solid Oxide Electrolytic Cell (SOEC) water acts like a reactant and it is fed from the cathode side of the cell. Oxygen ions are transported to the anode through the electrolyte and the hydrogen in produced cathode side (Figure 2.6).

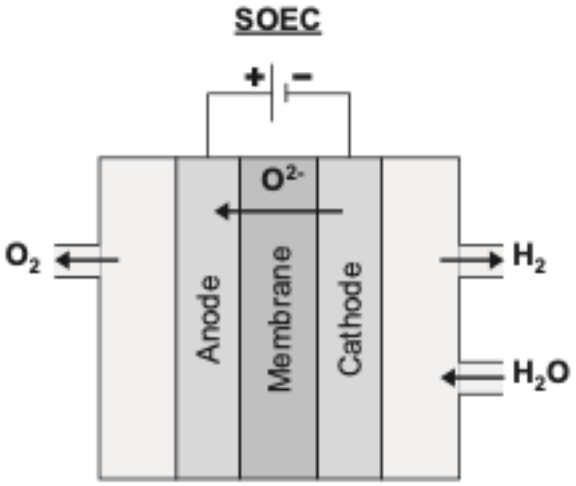

Figure 2.6: Conceptual design of a SOEC [12]

The overall reaction of water electrolysis, which allows to split water into hydrogen and oxygen supplying electrical and, if required, thermal energy is:

$$H_2O \longrightarrow H_2 + \tfrac{1}{2} O_2$$

While the semi-reactions which occur at the electrodes are, respectively for cathode and anode side:

$$H_2O + 2e^- \longrightarrow H_2\,(g) + O^{2-} \qquad Cathode$$

$$O^{2-} \longrightarrow \tfrac{1}{2} O_2\,(g) + 2e^- \qquad Anode$$

It is easy to notice that the volumetric co-production of oxygen corresponds to half of the production of hydrogen.

To avoid re-oxidation of the fuel electrode, a fraction of cathode exhausts can be recirculated, so the inlet stream to the cathode will contain a fraction of hydrogen.

The Reactant Ratio (RR) expresses the reactant molar fraction over the whole inlet molar flow.

Also, not all the reactant will react in the stack. In order to consider this phenomenon, the Reactant Utilization (RU) is used: it indicates which is the percentage of the total flow actually reacting in the stack.

The fraction of inlet molar flow which is actually converted ($\dot{n}_R$):

$$\dot{n}_R = \dot{n}_{IN} \cdot RU \cdot RR$$

The overall energy demand of reaction ΔH, can be partly supplied by heat (ΔQ), while another part (change in Gibbs energy ΔG) has to be supplied electrically:

$$\Delta H = \Delta G + \Delta Q$$

The minimum electric energy supply required for the electrolysis process is equal to the variation in the Gibbs free energy:

$$\Delta G = \Delta H - T \cdot \Delta S$$

Where ΔH is the enthalpy variation, T the temperature and ΔS the entropy variation.

The overall energy demand ΔH increases slightly with temperature (Fig. 2.7), but the electrical energy demand, ΔG, decreases with the increasing temperature: the ratio ΔG to ΔH is about 93% at 100°C and about 70% at 1000°C [26].

Operating at high temperatures can decrease the cost of the hydrogen produced: since the thermal energy required for the electrolysis reaction can be obtained from the Joule heat produced within the cell and the electrical demand is reduced at higher temperatures, the H_2 production price decreases.

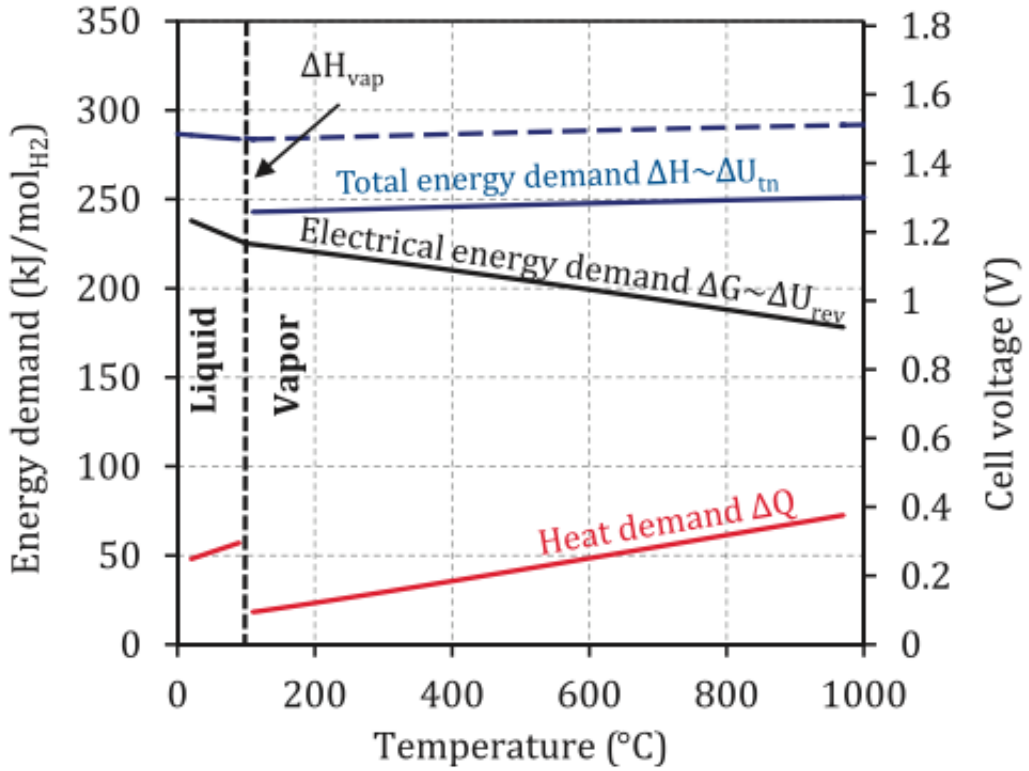

Figure 2.7: Total, thermal and electrical energy demand for an ideal electrolysis process as a function of T [27]

The thermoneutral potential is defined as the potential at which the generated Joule heat in the cell and the heat consumption for the electrolysis reaction are equal:

$$U_{tn} = \frac{\Delta H}{z \cdot F}$$

In other terms, it is the voltage at which thermal integration with an external source is not required and all the energy demand is supplied electrically. In a real electrolyser the cell voltage for thermoneutral operation is slightly higher than U_{tn} due to heat losses and thermodynamic irreversibilities. Typically, for a SOEC, this voltage is of around 1.29 V.

Operating below this value, the heat must be supplied to the cell to maintain the temperature (*endothermic mode*), while operating above this voltage, the cell operates in *exothermic mode* and the produced heat has to be extracted.

If H_2O is fed into the system in liquid phase, also the heat demand for water evaporation has to be considered and there will be an increase in the operation voltage [26]:

$$V_{vap} = \frac{\Delta H_{vap}}{z \cdot F}$$

The thermoneutral potential is then defined as the sum of both contributions:

$$U_{tn,liq} = \frac{\Delta H + \Delta H_{vap}}{z \cdot F}$$

The possible high heat utilisation of internal losses is one of the major motivation to operate high temperature electrolysis (at 700-900°C).

In general, low temperature electrolysers are operated above the thermoneutral voltage due to high internal losses or overvoltages. This results in a heating of the electrolysis cells requiring external cooling of the module.

For high temperature electrolysers, instead, thermoneutral voltage represents the standard operation mode. The cell is operated at constant temperature as internal heat production by irreversibilities is equalised by heat consumption of the electrolyser reaction.

2.4.1 Polarization curve

The relationship between voltage and current density is a fundamental characteristic of the cell efficiency.

The cell voltage can be expressed as the sum of the reversible cell voltage U_{rev}, also called Open Circuit Voltage (OCV) and the overvoltages caused by ohmic resistance U_{ohm}, limitations in electrode kinetics (activation overvoltages U_{act}) and mass transport (concentration or diffusion overvoltage U_{diff}):

$$U = U_{rev} + U_{ohm} + U_{act} + U_{diff}$$

First of all, the OCV (or U_{rev}) is the difference of potential between the two terminals of the cell when it is disconnected from any circuit. It can be estimated with the Nernst equation:

$$OCV = \frac{\Delta G}{z \cdot F}$$

Where ΔG is the Gibbs free energy variation, z the number of electrons involved in the reaction (which is 2, in this case) and F the Faraday constant.

As previously written, the operating voltage differs from OCV due to some irreversibilities which cause overvoltages within the cell:

- **Activation overvoltage (η_{act})**. It is due to two phenomena: the chemical equilibrium state of ions at the electrode-electrolyte interface and the overcoming of the electric field due to transfer of charged particles across the interface by ions. It can be decreased increasing temperature, active surface area or activity of the catalyst;

- **Ohmic overvoltage (η_{ohm})**. It is caused by the resistance to conduction of ions in the electrolyte, conduction of electrons in the electrode and contact resistance. Normally, only ionic resistance are considered, all the others are neglected;

- **Diffusion or concentration overvoltage (η_{diff})**. It is very relevant at high current densities, due to transport phenomena;

All the overvoltages previously described grow with the current density, but one of the mechanisms prevails over others depending on the operating zone.

The dependency between cell voltage and current (or current density) is shown in Figure 2.8 with a review of different SOEC characteristics from literature [27]. The current-voltage (I-U) curve characterises the electrochemical behaviour of an electrolysis cell.

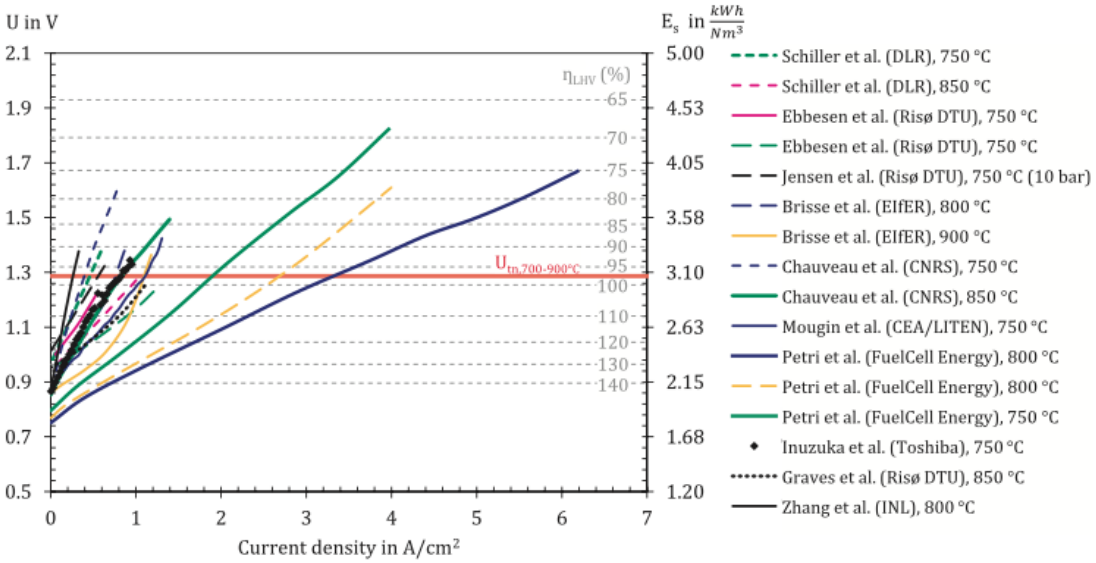

Figure 2.8: Overview of characteristic I-U curves of SOECs from literature [27]

A simplest model can be obtained assuming linear relationship between voltage and current density (*linearization of the polarization curve*).

This hypothesis is well justified for a SOEC since high temperatures enhance the kinetic of electrochemical reactions, increasing the reaction rate and decreasing the activation overvoltage, and improve the diffusion of reactants in electrodes, decreasing the diffusion overvoltage.

The slope of this first order curve is the **Area Specific Resistance (ASR)**, defined as:

$$ASR = \frac{V_C - OCV}{j}$$

Where V_C is the cell potential [V], j is the current density [A/m^2].

So the operating voltage can be expressed, as a function of current density in this way:

$$V_C = OCV + j \cdot ASR$$

ASR is influenced by materials used for the construction of the cell (both electrolyte and electrodes), geometrical features and operational parameters, like temperature, pressure and inlet gas composition [28].

2.4.2 Cell efficiency

The electrical power needed by the cell can be calculated as:

$$P_{el} = V_C \cdot j \cdot S$$

Where V_C is the cell potential, j the current density and S the active surface area of the cell [m^2].

The current density is proportional to the hydrogen production rate, as expressed by the Faraday's law, considering also the Faraday efficiency η_F (or current efficiency) which is defined as the ratio between actual hydrogen production rate and the theoretical one. For the modules, with n_c electrolysis cells and operating at current I, the total hydrogen production rate in Nm^3/h is then:

$$\dot{V}_{H_2} = \eta_F \cdot \frac{(n_C \cdot I)}{2 \cdot F} \cdot [2.414 \cdot 3.6 \frac{Nm^3}{mol} \cdot \frac{h}{s}]$$

And the efficiency of an electrolyser can be defined as

$$\eta_{HHV} = \frac{\dot{V}_{H_2} \cdot HHV_{H_2}}{P_{el}}$$

Where HHV_{H_2} is the Higher Heating Value of hydrogen (3.54 kWh/Nm^3) and P_{el} the electric energy consumption in kW. The cell voltage U_C given in V is inversely proportional to the efficiency:

$$\eta_{HHV} = \frac{\eta_F \cdot \frac{n_C \cdot I}{2 \cdot F} \cdot HHV_{H_2}}{n_C \cdot U_C \cdot I}$$

The electrolyser efficiency could also be referred to the lower heating value LHV_{H2} (3.00 kWh/Nm^3):

$$\eta_{LHV} = \frac{\dot{V}_{H_2} \cdot LHV_{H_2}}{P_{el}} = \frac{3.00}{3.54} \cdot \eta_{HHV} = \frac{1.25\ V}{U_C \cdot \eta_F}$$

It is also possible to define the specific energy consumption for the production of 1 Nm^3 (or 1 kg) of hydrogen, which is proportional to the cell voltage:

$$E_S = \frac{LHV_{H_2}}{\eta_{LHV}} = \frac{\eta_F \cdot U_C}{2.4V}$$

The efficiency of an electrolyser decreases:
- with increasing current density (and increasing U_c then);
- with decreasing temperature;
- slightly with increasing pressure.

2.4.3 Solid Oxide Electrolytic Cell (SOEC)

It is an electrolytic cell which operates at temperatures of 700-900°C. High temperature means higher efficiencies, but also that great attention has to be paid to the material stability. A simplified process layout of a Solid Oxide Electrolysis (SOE) system is shown in Figure 2.9 [27].

The feed water or steam is pre-heated in a recuperator against the hot product streams leaving the stack. Low temperature heat has to be integrated to account for the heat of evaporation. The stack consists typically of planar cells electrically connected in series. Steam and recycled hydrogen are supplied to the cathode to maintain reducing conditions and are partly converted to hydrogen. The mixture of steam and hydrogen is eventually separated by cooling and condensing the water.

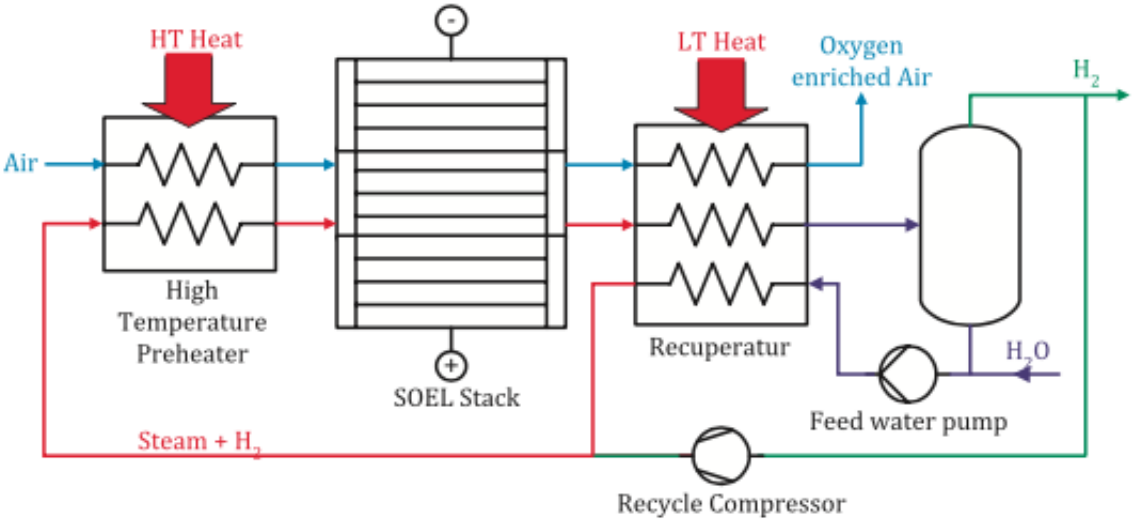

Figure 2.9: Simplified layout of a SOE system [27]

Air can be used at the anode as “sweep stream” for the removal of product oxygen. As demonstrated by Barelli et al. [29], it is possible to substitute air with steam on the oxygen electrode side as sweep gas, without any decrease in performance. It also gives the opportunity to produce pure oxygen without any further separation cost needed, since it is only necessary to condense water to separe it from oxygen, while if air is used as “sweep unit” as Air Separation Unit is necessary.

The sweep gas is needed because the anode, which is the oxygen electrode, presents the higher contributions to ohmic losses during the operations and the higher degradation due to delamination of the electrode/electrolyte interface. Also, high oxygen concentrations in the electrode increases polarization losses. So the function of the sweep gas is to “clean” the electrode flowing out the oxygen from the anode, reducing in this way the oxygen concentration.

In this work steam was preferred as sweep gas, since it is already available in the system for the production of hydrogen in the SOEC and because the gasifying agent needed in the gasification stage is a mixture of oxygen and steam.

2.4.4 SOEC materials

The most common electrolyte material is a dense ionic conductor, consisting of ZrO_2 doped with 8 mol% of Y_2O_3 (YSZ). This material presents high ionic

conductivity as thermal and chemical stability at the operation temperatures, which are of about 800-1000°C. For the fuel electrode (cathode), the most commonly used material is a porous cermet composed of YSZ and metallic nickel. While, for the oxygen electrode, the most used material is the lanthanum strontium manganite (LSM)/YSZ composite [26].

2.5 Syngas clean-up system

The raw syngas produced in the gasifier is rich of contaminants, mainly tars and other inorganic compounds, like nitrogeneous compounds (e.g. NH_3), sulfur containing compounds (e.g. H_2S) and hydrogen halogens (e.g. HCl).

Before being used in downstream applications, the raw syngas has to be cleaned then with different levels of purity required depending on the final purpose. There are two main possibilities to reach this goal: low temperature processes (**cold gas cleanup**) and mid-to-high temperature processes (**hot gas cleanup**) [30].

2.5.1 Cold gas clean-up

Cold gas clean-up is considered the conventional approach for syngas cleaning, due to its high contaminant removal efficiency. It is carried out at low temperature, which means at or even below ambient temperature.

The main disadvantage of this approach is the loss of efficiency due to the syngas cooling, since gasification is usually carried at high temperatures, in the range of 800-1200°C.

Cold gas cleanup utilizes “wet” or “dry” processes.

- Dry cold gas clean-up processes employ mechanical, physical and electrostatic separators, like cyclones, electrostatic precipitators and other filters.

- Wet cold gas clean-up processes, on the other hand, employ mainly spray and wash towers: these units remove contaminants by absorption and adsorption, filtration or a combination of them.

Wet cold gas cleanup processes are most commonly used, since they allow for multiple-contaminants removal. It is a very suitable solution especially for the inorganic contaminants. For example HCl, NH_3 and H_2S are very soluble in water, so wet towers or scrubbers using water as a solvent will remove all of these contaminants at varying removal efficiencies based on their solubility

in water. Further and more detailed informations about the cold gas clean-up methods and processes have been reported by Abdoulmoumine et al. [30].

2.5.2 Hot gas clean-up

Hot gas clean-up approach is of great interest in contaminant removal from syngas. It is carried out at temperatures higher than 300°C.

The main advantage of this solution is that it does not require to cool down the raw syngas, thus avoiding a loss in efficiency. It also reduces the waste streams with the potential of converting some contaminants into useful products [30].

There are two different solutions to reduce the tar content in syngas: **primary methods**, which are the methods operating directly during the gasification stage to limit tars formation, and **secondary methods**, also known as post-gasification methods, which operate downstream of gasification. Secondary methods involve physical, thermal or catalytic treatments [31].

Tar compounds can be removed mainly by thermal cracking and steam or dry reforming. Thermal cracking is the conversion of tar species into C and H_2 and it requires temperatures higher than 1100°C.

$$C_nH_m \longrightarrow nC + \tfrac{m}{2}H_2 \qquad Thermal\ cracking$$

Tar as well as light hydrocarbons can be converted to carbon monoxide (CO) and hydrogen (H_2) through steam reforming, as shown below

$$C_nH_m + nH_2O\,(g) \longrightarrow nCO + \tfrac{n+m}{2}H_2 \qquad Steam\ reforming$$

Steam reforming of tars occurs only above 900°C in the absence of a catalyst [30].

In any case, both these two solutions are better performed with the employment of a catalyst, directly into the gasifier.

The right choice of the catalyst is an important task. A good primary catalyst should have good activity for the conversion of tars into valuable gaseous products (e.g. H_2 and CO), but also good stability and resistance to attrition and deactivation through coking, sulfur poisoning or sintering [31].

Generally tar cracking and steam reforming reactions, as well as particulate removal, which is not considered in this model, are obtained in downstream components, like **ceramic catalytic filters** (or **candles**). These components might also be positioned in the freeboard of a BFB reactor, having the possibility to obtain a very compact unit. In this way it is also possible to combine hot gas filtration and cleaning from inorganic impurities with catalytic tar reforming in a single stage. Some of the used catalysts, in fact, act also as a primary sorbent for ammonia, hydrogen sulphide and hydrogen chloride. The mineral catalyst like dolomite (CaO-MgO) and olivine (Mg_2SiO_4-Fe_2SiO_4) and the nickel and iron based catalysts have been proven to be the most effective at temperatures raging from 500 to 900°C. [30].

Great attention has to be paid to other inorganic contaminants removal, since they are responsible for corrosion and other issues especially for the downstream equipments. It is important to consider one or more blocks to remove or reduce the contaminants concentration below the limits required for the final applications. The quasi-total removal of hydrogen sulphide at temperatures of about 400°C is obtained thanks to solid-gas reactions between the contaminant and a metal oxide (MO), especially Zn, Cu and Ce oxides. HCl is treated with alkali-based sorbents, like $NaHCO_3$, in the temperature range of 526-650°C. In both cases it is possible to reach contaminant concentrations of 1 ppm or lower [32].

2.6 Methanation

Methanation is a physical-chemical process which aims to produce methane from hydrogen and carbon oxides.
The two methanation reactions are:

$$CO + 3H_2 \longrightarrow CH_4 + H_2O\,(g) \qquad \Delta h^0 = -206\ kJ/mol \qquad CO\ methanation$$

$$CO_2 + 4H_2 \longrightarrow CH_4 + 2H_2O\,(g) \qquad \Delta h^0 = -164\ kJ/mol \qquad CO_2\ methanation$$

Both reactions are exothermic. For each 1 m^3 of methane produced per hour, 2.3 and 1.8 kW heat are produced respectively [33]. CO_2 methanation is a linear combination of CO methanation and reverse water-gas shift (RWGS) reaction, which always accompanies the CO methanation reaction using nickel catalysts.

$$CO_2 + H_2 \longrightarrow CO + H_2O\,(g) \qquad \Delta h^0 = 41 kJ/mol$$

The equilibrium of both reactions is influenced by pressure and temperature [33].

In thermodynamic equilibrium, high pressures favor the production of methane. High temperatures, on the other hand, limit methane formation. However, the performance becomes poor at temperatures below 200°C and too high pressures, because of reaction kinetics limitations.

The input gas for the methanation section must have a composition with the correct ratios between the reactants, which are CO, CO_2 and H_2.

The predominant methanation reaction is the CO methanation, which requires an H_2/CO = 3. But also CO_2 methanation has to be taken into account, so the feed gas has to meet the following stoichiometric requirement, which is called "**Feed Gas Module**":

$$FEED = \frac{y_{H_2} - y_{CO_2}}{y_{CO} + y_{CO_2}} = 3$$

Where y_i represents the molar fraction of the reactant i.

Catalytic methanation reactors are typically operated at temperatures between 200°C and 550°C and at pressure raging from 1 to 100 bar [34]. A catalyst is required to achieve acceptable rates and high selectivity. Several materials may be used, but the most common choice is represented by Ni, due to its availability and low cost. Nickel based catalysts require a high purity of the feed gas, so great attention has to be paid to syngas cleaning before it reaches the methanation section: in particular it is necessary to remove sulphurous compounds, which are responsible of sulphur poisoning. In this work, sulphur compounds are represented only by H_2S.
Methanation is a strongly exothermic reaction, so another big issue is to realise a good temperature control in the reactor, since high temperatures can cause catalyst sintering and carbon deposition. The chosen design consists in a series of cooled reactors with an intermediate condensation stage in order to condense and remove the produced water.

Chapter 3

Process modelling

3.1 General aspects

The commercial software ASPEN Plus was used to model the plant. It is a process modelling tool for conceptual design, optimization and performance monitoring of chemical processes.

It has a huge database of pure components and phase equilibrium data for conventional chemicals, electrolytes, solids and polymers and with reliable thermodynamic data, so it is possible to simulate the actual plant behavior, using some engineering relationships, physical and chemical laws, such ass mass and energy balances, phase and chemical equilibrium and reaction kinetics.

In this work, the hypothesis of chemical equilibrium was applied to all the reactors, but the User2 block which represents the gasification stage [35, 36, 37].

The stream class **MIXCINC** was selected. Stream classes are used to define the structure of simulation streams. The selected one includes:

- **Conventional streams (MIXED)**, i.e. vapour/gas and liquid streams and solid salts in solution chemistry;
- **Conventional inert solids (CI)**, i.e. solids that are inert to phase equilibrium and salt precipitation/solubility, but take part to chemical equilibrium (using Gibbs reactors);
- **Non-conventional solids (NC)**, i.e. heterogeneous substances inert to phase, salt and chemical equilibrium that cannot be represented with a molecular structure.

To calculate non-conventional solids properties, it is necessary to specify the “NC Props”. The only physical properties needed in this case are enthalpy and density.

This is done using the HCOALGEN and the DCOALIGT models. In particular, the HCOALGEN uses the proximate analysis, the ultimate analysis and the sulphur analysis to calculate the enthalpy of the non-conventional solid considered.

All the values of proximate, ultimate and sulphur analysis are defined as weight percentage on a dry basis, with the exception of moisture in proximate analysis, which is expressed clearly on wet basis.

The sum of the values of the sulphur analysis must be equal to the value for sulphur specified in the ultimate analysis.

The value specified for ash must be equal for ultimate and proximate analysis.

The sum of the values specified for ultimate and for the proximate analysis must be equal to 100 in both cases.

All the components used in this work were specified:

- BIOMASS and ASH as NC;
- C as conventional inert solid;
- H_2O, CO, CO_2, CH_4, H_2, O_2, $C_3H_6O_2$, C_7H_8, C_6H_6, C_6H_6O, $C_{10}H_8$, NH_3, H_2S, HCl, N_2 as conventional streams.

Finally, the thermodynamic methods used to calculate the properties of the conventional streams were selected:

- The **IDEAL** property method (Ideal gases, Raoul’s Law and Henry’s Law) was selected for the drying and gasification section;
- The **PENG-ROB** property method (Peng Robinson equation of state) was selected for all the other sections.

A simplified process flowchart is reported in Figure 3.1.

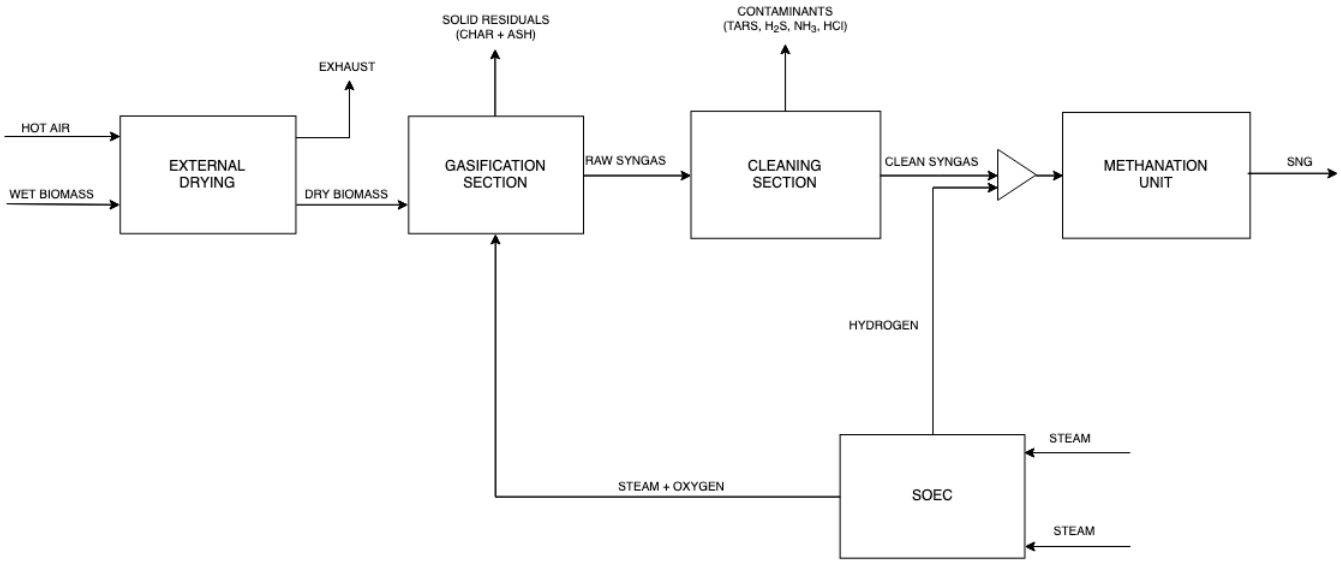

Figure 3.1: Simplified process flowchart

3.2 External drying section

The simulation model of the external drying section is shown in Figure 3.2. The as-received stream of biomass is fed to the drier both with an hot air stream at T = 150°C.

A biomass stream with reduced moisture content (DRY-BIO) and a stream of moist air (EXHAUST) are the output of the drier.

The model uses two-unit operation blocks, which are a RStoic and a Flash2 block, to simulate a single piece of equipment. For this reason, the extra stream that connects the two simulation blocks ("IN-DRIER") has not a real physical meaning.

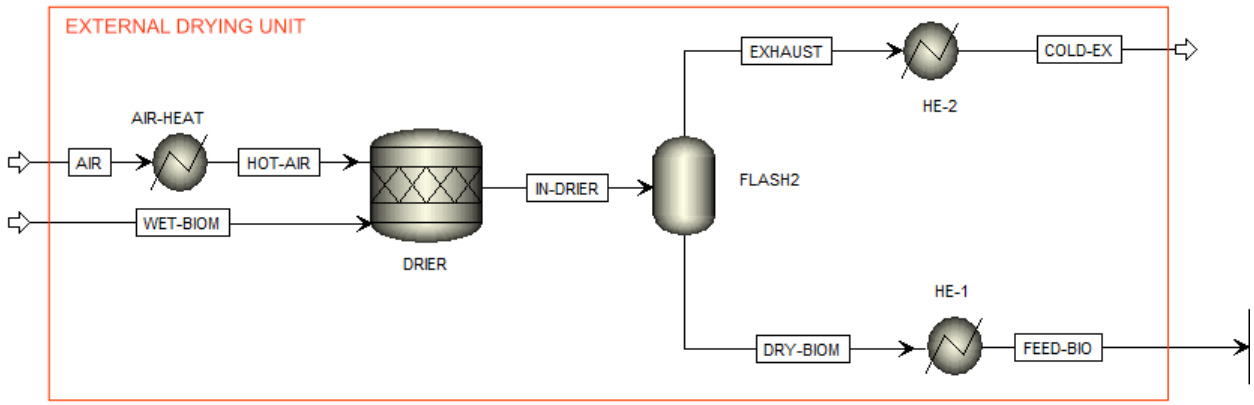

Figure 3.2: External drying unit flowsheet

The drier is modeled with an RStoic block ("DRIER"), in which a portion of biomass reacts to form water. Since the RStoic block has a single outlet stream, a Flash2 block ("FLASH2") is used to separate the dried biomass from the moist air.

The drier and the separator are supposed to be adiabatic and pressure drops are set to be equal to 0.

The equation which simulates the biomass drying is:

$$BIOMASS \longrightarrow 0.0555084 \cdot H_2O$$

This is only a temporary value which is overwritten then by means of a Calculator Block ("WATER"). It allows to specify the moisture content of the dried biomass and to calculate the corresponding fractional conversion of the biomass to water. The fractional conversion is calculated considering the following mass balance equations applied to the moisture content and to the

overall biomass:

$$\dot{m}_{wetbiomass} \cdot \frac{H_2O_{in}}{100} = \dot{m}_{drybiomass} \cdot \frac{H_2O_{out}}{100} + \dot{m}_{wetbiomass} \cdot CONV$$

$$\dot{m}_{wetbiomass} = \dot{m}_{drybiomass} + \dot{m}_{wetbiomass} \cdot CONV$$

where
$\dot{m}_{wetbiomass}$ is the mass flow rate of the inlet biomass [kg/s];
$\dot{m}_{drybiomass}$ is the mass flow rate of the inlet biomass [kg/s];
H_2O_{in} is the weight percentage of moisture of the inlet biomass;
H_2O_{out} is the weight percentage of the moisture of the outlet biomass;
$CONV$ is the fractional conversion of biomass to water.

Combining these two equations, it is possible to obtain an expression for the fractional conversion:

$$CONV = \frac{H_2O_{in} - H_2O_{out}}{100 - H_2O_{out}}$$

By imposing a weight percentage of moisture of the outlet biomass (a value chosen by the user), it is possible to calculate the fractional conversion that will be assigned to the drier block.

In this work, as base case, the residual moisture percentage was set equal to 8% for the outlet biomass flow ("DRY-BIOM").

3.3 Gasification section

The figure below (Figure 3.3) shows the simulation model of the gasification section.
The dried biomass exiting from the previous section is sent to the gasifier, while the final product is represented by the syngas and the solid residuals, which are the not-reacted char and ash.

Also in this case, more components are used to simulate a single piece of equipment, so all the extra streams which connect the simulation blocks have not a physical meaning actually.

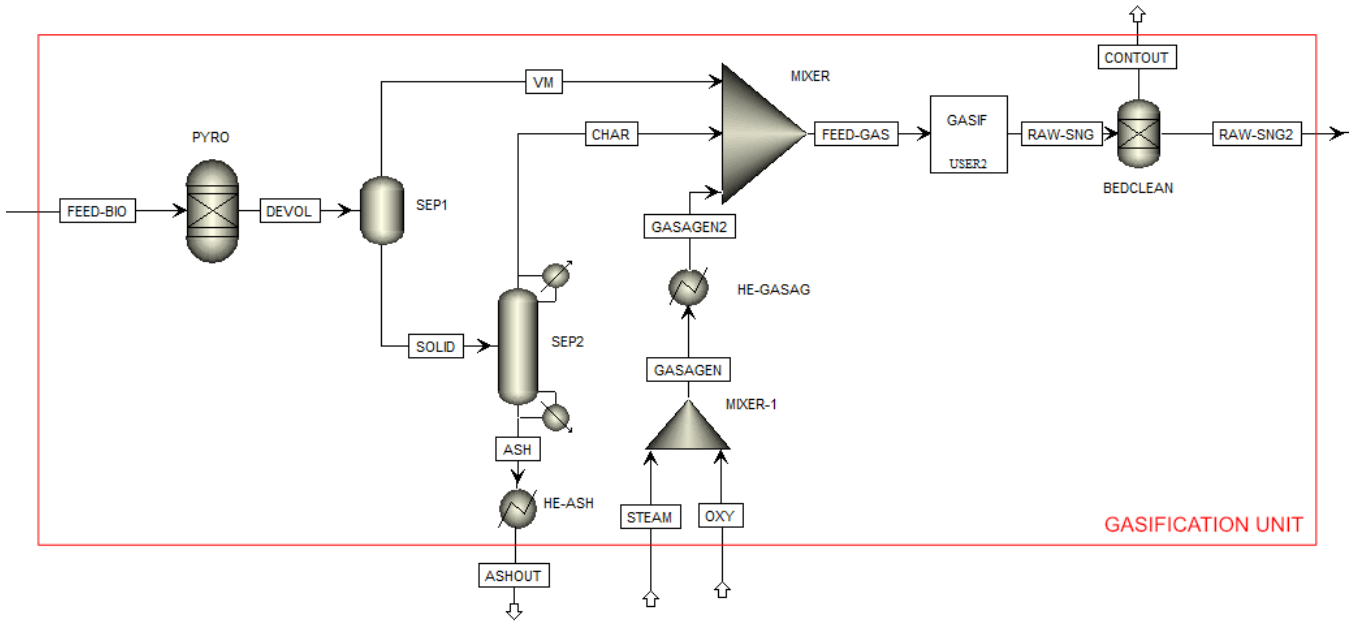

Figure 3.3: Gasification unit flowsheet

Gasification could be simulated with two different approaches:

- **Equilibrium model**
  It is a a zero dimensional model, so it is space independent and it is helpful in identifying the maximum possible conversion of biomass and the theoretical efficiency. It cannot be used for reactor analysis and design because it can only predict the end-reaction product distribution and cannot describe the instantaneous product distribution along with the geometric dimensions. It is used to predict maximum achievable yield of a desired product from a reacting system [3]. It is important to say that these ideal yields could never be reached, due to a limited

residence time in the reactor which does not allow to reach equilibrium conditions. This approach was adopted by Giglio et al. [9];

- **Kinetic model**
  It is used to predict the progress and the product compositions at different positions along the reactor. It is a 1 dimensional model, which takes into account also the geometry of the reactor, especially in terms of height and diameters. In general, these models give a better accuracy in terms of composition of the raw syngas.

In this work, this second approach was chosen, aiming to improve Giglio et al. model in terms of gasification syngas composition predictions.
As previously said, gasification can be considered as made up by three different stages, which are devolatilization, oxidation and reduction. They are modeled in this work with different components and in subsequent moments, but it has to be kept in mind that all the phenomena modeled and described in the following paragraphs actually happen in the same time and in the same component, which is a Bubbling Fluidized Bed Gasifier.

3.3.1 Literature review

Some models, described by other authors in the literature, were taken as main references.

Campoy et al. (2008) performed several tests in a bubbling fluidized-bed (BFB) gasification power plant. They studied the effect of steam addition as gasifying agent on the performances of gasification. The reactor was operated near adiabatic conditions. The temperature of the gasifying agent was set at 400°C, a value that can be achieved by energy recovery from the output gas without tar-condensing problems. SBR and ER were varied in a certain range and the experimental results were reported [10].

Nikoo et al. (2008) developed a comprehensive process model for biomass gasification in a fluidized bed reactor using the ASPEN Plus simulator. They considered both hydrodynamic parameters and reaction kinetic modeling, by means of an external FORTRAN subroutine to simulate the gasification process [38].

Pauls et al. (2016), improved Nikoo's model including new interesting features. A temperature-dependent pyrolysis model has been added, based

on the use of empirical temperature-dependent equations, which take into account also the tar formation. The hydrodynamic model has been improved too and more extensive gasification kinetics were considered, with the inclusion of gasification homogeneous reactions and tar cracking reaction kinetics [39].

Kaushal et al. (2010, 2017) followed a similar path. In these works a semi-kinetic approach was used to model devolatilization process, using Arrhenius type kinetic model to define devolatilized-gas composition. These models also consider tar formation and cracking, but they are not very clear about the species which have been chosen to represent tar and generic "tar_1" and "tar_{inert}" are used to represent primary and secondary tars [40, 41].

Miao et al. (2012) modeled biomass gasification in circulating fluidized bed, starting from a review of previously existing models. This work has been considered as reference especially for the set of gasification reaction kinetics, made up by 8 different equations, both heterogeneous and homogeneous [20].

Dang et al. (2020) finally built a kinetic model for prediction and optimization of syngas production. The pyrolysis step is modeled with a one-step global model, based on elemental balances and on the imposition of the molar ratio CO/CO_2 as additional constrain. The model predictions have been compared with experimental results from Campoy et al. (2008), and the results showed a good agreement under a wide range of operating conditions [11].

Gomez-Barea et al. (2013) applied a quasi-equilibrium model (QEM) to improve the accuracy of the prediction of the gas composition with respect to an equilibrium model. The approach was first used by Gumz (1951), who introduced the "quasi-equilibrium temperature" concept [42].

3.3.2 Devolatilization modelling

Assumptions

The devolatilization process was assumed to be instantaneous, due to the fast heating rates within a fluidized bed reactor, and to occur at nearly gasification temperature [39]. The one-step global model approach was applied.

During the pyrolysis stage, four main species are formed:

- Char, made up by solid carbon and inert ash;
- Non-condensable gases, which are assumed to be CO, CO_2, CH_4, H_2, NH_3, H_2S, HCl;
- Tar, represented in this work, in this stage, by $C_3H_6O_2$ and C_7H_8;
- Water, which is equal to the moisture percentage of the biomass entering the "pyrolysis" stage.

For the tar formation, experimental results indicate that the tar content is generally less than 2 wt% with high gasifier temperature of 850°C and more [11].
In Campoy experimental results [10] it is reported that tar yield is roughly 4 $g/kg_{d.a.f.,biomass}$, with a reaction temperature of about 800°C.
Due to this considerations, it was assumed as tar yield during the pyrolysis stage a value of 5 $g/kg_{d.a.f.,biomass}$, as a precautionary value which overestimates the tar production.

Devolatilization modelling

Devolatilization (or pyrolysis) was modeled with a RYield block (called “PYRO”), used to specify the mass yields of the considered product species, which were listed in the "Assumptions" paragraph.

Default initial values are overwritten with the values obtained with a Calculator Block (“PYROL”). This step is assumed to occur at 700°C.

The outlet stream (“DEVOL”) is a mixture of solid (char and ash) and gaseous species, both condensable and non-condensable ones.
It is hard to determine the exact product composition after the pyrolysis stage. In this work a one-step global model was employed.
Char yield is taken from the proximate analysis, considering fixed carbon and ash percentages, since it was assumed that char is made up by these two species.

Tar yield is assumed to be 5 wt%, as discussed before. Tars are represented by two species during this stage: 1-hydroxy-2-propanone ($C_3H_6O_2$) and toluene (C_7H_8), each with a specific yield of 50 wt% tar. These two compounds will react during the next stage, where their cracking reactions are

modeled.

Some of the non-condensable gases generated during this phase are assumed to not participate during the oxidation and reduction stage, so they are considered as “inerts”. These gases are the N, S and Cl compounds, which are assumed to be represented only by NH_3, H_2S and HCl respectively [30]. Knowing the biomass composition in terms of N, S and Cl content, from its ultimate analysis, an elemental balance is performed to define the mass yields on dry basis of the three gaseous species considered as inerts. First of all the mass flows of the single elements are calculated, knowing the biomass mass flow, the ultimate analysis and the moisture content of the biomass

$$\dot{m}_N = FACT \cdot \frac{ULT_N}{100} \cdot \dot{m}_{biomass}$$

$$\dot{m}_S = FACT \cdot \frac{ULT_S}{100} \cdot \dot{m}_{biomass}$$

$$\dot{m}_Cl = FACT \cdot \frac{ULT_Cl}{100} \cdot \dot{m}_{biomass}$$

Where
$FACT$ = (100-$MOIST$)/100 is the correction factor used to refer to the dry biomass mass flow;
ULT_i is the mass weight percentage of the i-th element taken from the ultimate analysis;
$\dot{m}_i$ is the mass flow of the i-th component [kg/s].

Knowing this values, it is possible to calculate the mass flows of the inert gases, then their mass yields.

$$\dot{m}_{NH_3} = \dot{m}_N \cdot \frac{MW_{NH_3}}{MW_N} \longrightarrow x_{NH_3} = \frac{\dot{m}_{NH_3}}{\dot{m}_{dry,bio}}$$

$$\dot{m}_{HCl} = \dot{m}_{Cl} \cdot \frac{MW_{HCl}}{MW_{Cl}} \longrightarrow x_{HCl} = \frac{\dot{m}_{HCl}}{\dot{m}_{dry,bio}}$$

$$\dot{m}_{NH_3} = \dot{m}_S \cdot \frac{MW_{H_2S}}{MW_S} \longrightarrow x_{H_2S} = \frac{\dot{m}_{H_2S}}{\dot{m}_{dry,bio}}$$

Finally, it is possible to determine the non-condensable gases composition, by mean of some elemental balance equations and of a further constrain, which is the initial molar ratio CO/CO_2.
About this last parameter, Dang et al. [11] performed a sensitivity analysis to

understand how the syngas composition changes by varying the molar ratio CO/CO_2 in a range of values from 0.5 to 2.0.
It was shown that the predicted final gas composition does not change much after the kinetic model calculations and iterations in the different cases, so in this work a value of CO/CO_2 equal to 1 was set for simplicity.
First of all, a molar balance of the residual elements is performed.

$$C_{res} = C_{ULT} - C_{char} - C_{C_3H_6O_2} - C_{C_7H_8}$$

$$H_{res} = H_{ULT} - H_{NH_3} - H_{H_2S} - H_{HCl}$$

$$O_{res} = O_{ULT} - O_{C_3H_6O_2}$$

Having set the initial CO/CO_2 molar ratio, and knowing the residual oxygen moles, it is possible to determine the number of moles of CO and CO_2:

$$CO_{mol} = \frac{O_{res,mol}}{3}$$

$$CO_{2,mol} = \frac{O_{res,mol}}{3}$$

The same thing is now done on the residual carbon and hydrogen moles and in this way it is possible to determine the number of moles of CH_4 and H_2:

$$CH_{4,mol} = C_{res,mol} - CO_{mol} - CO_{2,mol}$$

$$H_{2,mol} = \frac{H_{res} - 4 \cdot CH_{4,mol}}{2}$$

And finally it is possible to determine the mass yields of the single gaseous species.

$$\dot{m_{CO}} = CO_{mol} \cdot MW_{CO} \longrightarrow x_{CO} = \frac{\dot{m}_{CO}}{\dot{m}_{biomass}}$$

$$\dot{m}_{CO_2} = CO_{2,mol} \cdot MW_{CO_2} \longrightarrow x_{CO_2} = \frac{\dot{m}_{CO_2}}{\dot{m}_{biomass}}$$

$$\dot{m}_{CH_4} = CH_{4,mol} \cdot MW_{CH_4} \longrightarrow x_{CH_4} = \frac{\dot{m}_{CH_4}}{\dot{m}_{biomass}}$$

$$\dot{m}_{H_2} = H_{2,mol} \cdot MW_{H_2} \longrightarrow x_{H_2} = \frac{\dot{m}_{H_2}}{\dot{m}_{biomass}}$$

All these calculations are performed with the Calculator block, which overwrites the default values given to the RYield block.

These products are the feed stream for the oxidation and reduction phases, which will be discussed later.

3.3.3 Gasifier modelling

3.3.3.1 ASPEN Plus model

This section represents mainly the oxidation and reduction zones, but it will be called generally “gasification” zone, for simplicity.

The gasification zone is modeled by mean of a User Defined Block User2 (“GASIF”), coupled with an external FORTRAN subroutine, used to model the hydrodynamic and kinetic behavior of the reactor.
The User2 block requires the following input parameters:
- Gasification temperature;
- Number of orifices of the distributor plate;
- Bed diameter;
- Bed height;
- Freeboard diameter;
- Maximum height, given by the sum of bed and freeboard height.

Feed of this block are: char and volatile matter from the devolatilization stage and the gasifying agent, which is a mixture of oxygen and steam, coming from the electrolysis section which will be discussed later. All these streams are mixed with a mixer (“MIXER”) before entering the “GASIF” block.

Ashes are separated with a Sep2 block (“SEP2”) from the devolatilization products since they are assumed to be inert and to not participate in any reaction. However, since they are actually in the reactor, they are heated up to the gasification temperature with an heater (“HE-ASH”).

As a product from this stage there will be the raw syngas - with all its contaminants and with a certain molar composition - and eventually some solid residuals (like unreacted char particles and bed material particles), which will be separated downstream by a solid separator in the following sections.

A separator (“BEDCLEAN”) is also added downstream, in order to consider the cleaning effect of the dolomite, which is used as catalyst in the reactor. It does not take part in the chemical reactions, but its adsorption effect over the inorganic contaminants is considered by mean of this separator. Different separation yields are specified for the different pollutant species,

which can be considered another output of the system (“CONTOUT”).
This is a very simplifying assumption: it is assumed that a certain percentage of contaminants is just separated from the produced syngas stream, without taking into account all the mechanisms and reactions actually happening within the catalyst and the gaseous species. All the specified separation yields are taken from the literature [32].

3.3.3.2 Hydrodynamics

Some simplifying assumptions are needed, since a fluidized bed is a complex system to be described:

- The bubbling fluidization regime is considered;
- It is possible to distinguish two main regions within the reactor: dense bed and freeboard;
- Variations in hydrodynamics occur in the axial direction only (mono-dimensional model);
- Effects from mass transfer are assumed to be negligible [39];
- Two-phase theory. In the dense bed two phases co-exist: emulsion phase and bubbling phase;
- Bubble diameter assumed to be constant and equal to the initial bubble diameter within the dense bed region [43];
- Mean voidage in the freeboard is assumed to be constant and equal to 0.75 [11].

3.3.3.2.1 Two phase theory When the bed is fluidized with a gas, and its velocity exceeds the minimum fluidization one, the bed can be treated as if it is made up by two phases: bubbles, in which it is assumed there are no solid particles, and an emulsion phase in which there is a condition similar to the minimum fluidization one.

3.3.3.2.2 Dense bed As discussed in Section 2.3.1.2 (“Fluidized bed reactors”), granular solids of a material, called bed particles, are kept in a semi-suspended condition (*fluidization*) in the reactor.
The main properties of these particles, for this work, are [11]:

$d_p = 0.25\ mm$ *Particle diameter*

$\rho_p = 2650\ kg/m^3$ *Particle density*

These two properties are used to determine some hydrodynamic parameters, with some equations given by Kunii and Levenspiel [44].
First of all, the Archimedes number (Ar) is calculated:

$$Ar = \frac{d_p^3 \cdot \rho_g \cdot (\rho_p - rho_g) \cdot g}{\mu_g^2}$$

Where
d_p is the bed material particle diameter [m];
ρ_g is the fluidizing gas density [kg/m^3];
ρ_p is the bed material particle density [kg/m^3];
g is the gravitational acceleration, equal to 9.81 m/s^2;
μ_g is the fluidizing gas viscosity [Pa·s].

This value is used to obtain the minimum fluidization velocity (u_{mf}), which is the minimum velocity to achieve the state of fluidization when a fixed bed of particles encounters a fluid in vertical direction. The u_{mf} is the minimum velocity required to overcome gravitational forces and break up the bed.

$$u_{mf} = \frac{\mu_g}{\rho_g \cdot d_p} \cdot \sqrt{27.2^2 + 0.0408 \cdot Ar} - 27.2$$

Knowing the Archimedes number, it is also possible to determine the porosity at minimum fluidization, which is the voidage in the emulsion phase (ε_{mf}) [40, 41].

$$\varepsilon_{mf} = 0.478 \cdot Ar^{-0.018}$$

Another important parameter to be determined is the bubble size, which affects the bubble rise velocity and then the volume fractions of the bubble and emulsion phases respectively.
Bubbles form when the fluidizing gas velocity exceeds the minimum fluidization velocity. Bubbles have an initial diameter which is influenced by the distributor plate's orifices dimension. Moving along the axial direction, as they rise up in the bed, they grow and coalesce.
In this work a simplifying assumption was done: the initial bubble diameter is assumed to stay constant along the axial direction, so there are no changes

in the fraction of bed occupied by the bubble and the emulsion phase in the axial direction.

The initial bubble diameter, d_{b0}, is dependent on the type of the distributor plate and, in particular, from the number of orifices (N_D), if it is a perforated plate as in this case. It can be estimated with the following equation provided by Mori and Wen [45]:

$$d_{b0} = 0.347 \cdot (A_t \cdot \frac{(u_0 - u_{mf})}{N_D})^{0.4}$$

Where
A_t is the cross-sectional area of the fluidized bed [cm^2];
u_0 is the superficial gas velocity [cm/s];
u_{mf} is the minimum fluidization velocity [cm/s];
N_D is the number of orifices of the distributor perforated plate [-].

Then it is possible to obtain the bubble rise velocity (u_b), which is used to calculate the fraction of bed occupied by the bubbles (δ_b) [44].

$$u_b = (0.71 \cdot \sqrt{g \cdot d_b}) + u_0 - u_{mf}$$

$$\delta_b = \frac{Y \cdot (u_0 - u_{mf})}{u_b}$$

Where Y is a correction factor set equal to 0.75 [11].

Finally it is possible to determine the average bed voidage, as the average fraction occupied by the gas within the dense bed, as:

$$vbed_{ave} = 1 - (1 - \delta_b) \cdot (1 - \varepsilon_{mf})$$

3.3.3.2.3 Freeboard The mean voidage in the axial direction varies along its length and it could be estimated with an exponential decay function [44]:

$$(1 - \varepsilon_f)_{fb} = (1 - \varepsilon_f) \cdot exp(-a \cdot h)$$

Where
a = 1.8/u_0;
ε_f is the volume occupied by the emulsion phase;
fb index refers to the freeboard.

In this work a simplicity approach is chosen, as done by Dang et al.: the freeboard mean voidage is assumed to be constant and equal to 0.75 [11].

The mean voidage is a very important parameter for the reaction kinetics, both in the dense bed and the freeboard, since each reaction has to be multiplied by the void volume, in order to represent the gas space within the bulk [39].

3.3.3.3 Chemical reaction kinetics

Some assumptions were introduced within the gasification model:

- One-dimensional fluidized bed reactor: variations occur in the axial direction only and perfect mixing in the radial direction;
- All the gases are uniformly distributed within the emulsion phase;
- Reactions are at steady state;
- The process is isothermal and the temperature is uniform within the reactor;
- Char particle size remains constant during the gasification process (shrinking core model);
- Char is pure carbon. Other elements content is neglected;
- Char gasification starts in the bed and completes in the freeboard;
- Ash is inert and does not participate in or affect any reactions;
- Gasification processes are assumed to be kinetically driven;
- Tar reactions are based on five representative species ($C_3H_6O_2$, C_7H_8, C_6H_6O, $C_{10}H_8$, C_6H_6);
- NH_3, H_2S and HCl are inerts and do not participate in any reaction.

The reaction kinetic expressions were taken from the literature and especially from Pauls [39], Miao [20] and Dang [11]. All the expressions used are reported in Table 3.1.

The reactor domain – and in particular its height, which is the only direction considered as previously written - is discretized in small increments (h_{inc}), so in small incremental volumes (v_{inc}), always keeping in mind that variations occur in the axial direction only.

For each incremental step, it is defined the concentration of the chemical species present within the reactor.
For gaseous components the concentration can be calculated from the ideal gas law:

$$C_i = \frac{p_i}{R_{gas} \cdot T}$$

Where
C_i is the i-th species concentration [kmol/m^3];
p_i is the i-th species partial pressure [Pa];
R_{gas} is the ideal gas constant [kJ/(kmol K)];
T is the gasification temperature [K].

Once the reaction rate is calculated, it has to be multiplied by the incremental volume, in order to obtain the reacting molar flow for the given discrete step, expressed in kmol/s.
Finally, it is possible to determine the molar flow – and so the concentration – of a given species in the following step, with simple balances:

$$n_{i,step+1} = n_{i,step} - \sum n_{i,step,reactant} + \sum n_{i,step,product}$$

Where
$n_{i,step+1}$ is the molar flow of the i-th species in the next incremental step [kmol/s];
$n_{i,step}$ is the molar flow of the i-th species in the considered incremental step [kmol/s];
$n_{i,step,reactant}$ is the molar flow of the i-th species that reacted in the considered step [kmol/s];
$n_{i,step,product}$ is the molar flow of the i-th species produced in the considered step [kmol/s].

The char molar flow is used also to determine the **carbon conversion factor** (**X**) in each stage, expressed as:

$$X = \frac{n_{char,t} - n_{char,0}}{n_{char,0}}$$

Where
$n_{char,t}$ is the char molar flow in the t-th step [kmol/s];
$n_{char,0}$ is the char initial molar flow [kmol/s].

Finally, the final composition of the raw syngas is determined at the exit of the reactor.

Chemical reaction rates			
No.	Stoichiometry	Reaction rate	Ref.
R1	$C + \frac{\lambda+2}{2\cdot(\lambda+1)} \cdot O_2 \longrightarrow \frac{\lambda}{\lambda+1} \cdot CO + \frac{1}{\lambda+1} \cdot CO_2$ $\lambda = 70 \cdot exp(-\frac{3070}{T_K})$	$r = 1.48 \cdot 10 \cdot exp(-\frac{13078}{T_K} \cdot p_{O_2} \cdot (1-X)^{1.2} \cdot C_C$	[39]
R2	$C + H_2O \longrightarrow CO + H_2$	$r = 200 \cdot exp(-\frac{6000}{T_K}) \cdot C_C \cdot C_{H_2O}$	[20]
R3	$C + CO_2 \longrightarrow 2 \cdot CO$	$r = 4.364 \cdot exp(-\frac{29844}{T_K}) \cdot C_{CO_2}$	[20]
R4	$CO + 0.5 \cdot O_2 \longrightarrow CO_2$	$r = 1.00 \cdot 10^{10} \cdot exp(-\frac{126000}{R_{gas} \cdot T_K}) \cdot C_{CO} \cdot C_{O_2}^{0.5} \cdot C_{H_2O}^{0.5}$	[11]
R5	$H_2 + 0.5 \cdot O_2 \longrightarrow H_2O$	$r = 2.19 \cdot 10^9 \cdot exp(-\frac{13127}{T_K}) \cdot C_{H_2} \cdot C_{O_2}$	[20]
R6	$CO + H_2O \longrightarrow H_2 + CO_2$	$r = 2.78 \cdot 10^6 \cdot exp(-\frac{1510}{T_K}) \cdot ((C_{CO} \cdot C_{H_2O}) - \frac{C_{CO_2} \cdot C_{H_2}}{k_6}$ $k_6 = 0.0265 \cdot exp(\frac{3968}{T_K})$	[11]
R7	$CH_4 + H_2O \longrightarrow CO + 3 \cdot H_2$	$r = 3.00 \cdot 10^{11} \cdot exp(-\frac{125000}{R_{gas} \cdot T_K}) \cdot C_{CH_4} \cdot C_{H_2O}$	[11]
R8	$CH_4 + 1.5 \cdot O_2 \longrightarrow CO + 2 \cdot H_2O$	$r = 1.585 \cdot 10^7 \cdot exp(-\frac{24157}{T_K}) \cdot C_{CH_4}^{0.7} \cdot C_{O_2}^{0.8}$	[20]
R9	$C_3H_6O_2 \longrightarrow 0.5 \cdot 0.5 \cdot C_6H_6O + 1.5 \cdot H_2O$	$r = 1.00 \cdot 10^7 \cdot exp(-\frac{136000}{R_{gas} \cdot T_K}) \cdot C_{C_3H_6O_2}$	[39]
R10	$C_6H_6O \longrightarrow 0.5 \cdot C_{10}H_8 + CO + H_2$	$r = 1.00 \cdot 10^{10} \cdot exp(-\frac{100000}{R_{gas} \cdot T_K}) \cdot C_{C_6H_6O}$	[39]
R11	$C_{10}H_8 \longrightarrow 10 \cdot C\,(s) + 4 \cdot H_2$	$r^* = 7.00 \cdot 10^{14} \cdot exp(-\frac{360000}{R_{gas} \cdot T_K}) \cdot C_{H_{2,m}}^{-0.7} \cdot C_{C_{10}H_{8,m}}^2$	[39]
R12	$C_7H_8 + H_2 \longrightarrow C_6H_6 + CH_4$	$r^* = 3.3 \cdot 10^{10} \cdot exp(-\frac{247000}{R_{gas} \cdot T_K}) \cdot C_{H_{2,m}}^{0.5} \cdot C_{C_7H_{8,m}}$	[39]

Table 3.1: Gasification chemical reaction rates

In Table 3.1, r is expressed in kmol/(m^{3}s) and r* in mol/(m^{3}s).

3.3.3.4 Model validation

The gasification model was first validated with the experimental results reported by Campoy et al. [10].
Also a comparison with the results obtained by Dang et al. [10] was done. In order to do this, the following geometrical input parameters were set for the User2 block, taken from the literature references:

- Bed diameter: 0.15 m;
- Bed height: 1.40 m;
- Freeboard diameter: 0.25 m;
- Total reactor height: 3.55 m;
- Number of orifices in the distributor plate: 32.

In the validation phase, a mixture of air and steam was considered as gasifying agent.

The validation was done considering the same biomass composition and flows of Dang's work (Table 3.2) [11].

Proximate analysis	% wt.	Ultimate analysis	% wt.
Moisture	6,30	Carbon	50,76
Fixed Carbon	16,68	Hydrogen	5,92
Volatile Matter	76,52	Nitrogen	0,00
Ash	0,50	Chlorine	0,00
		Sulfur	0,00
		Oxygen	43,32

Table 3.2: Biomass composition used for model validation

The predictions of the model were compared with the results reported by Campoy and Dang by mean of the **Round Mean Square Error** (**RMSE**), defined as:

$$RMSE = \sqrt{\frac{1}{N} \cdot \sum_{i=1}^{N} (Y_i^{ref} - Y_i^{model})^2}$$

Where
N is the number of changing parameters (in this case equal to 4, since we consider the molar composition in terms of CO, CO_2, CH_4 and H_2;
Y_i^{ref} is the molar fraction of the i-th species reported by the reference (Campoy or Dang, in this case);

Y_i^{model} is the molar fraction of the i-th species predicted by this model.

A set of values reported by Dang were used to compare the model results, as reported in the table below (Table 3.3).

Variables		SET 1	SET 2	SET 3	SET 4	SET 5
ER		0,34	0,32	0,32	0,26	0,26
SBR		0	0,22	0,45	0,23	0,43
$T_{gas,set}$ [°C]		800	800	780	780	750
CO $(\%\ vol.)*$	Experimental	35,3	32,1	28,3	30,1	22,9
	Dang et al., 2020	33,3	29,56	22,7	28,47	19,59
	Model	32,8	27,9	21,98	29,13	22,24
H_2 $(\%\ vol.)*$	Experimental	19,5	24,8	27,3	28,1	31,2
	Dang et al., 2020	20,03	29,31	32,72	29,69	31,98
	Model	19,84	28,71	32,83	31,38	34,26
CO_2 $(\%\ vol.)*$	Experimental	33,8	33,1	34,9	32,5	35,8
	Dang et al., 2020	35,25	33,05	37,12	32,1	38,44
	Model	33,72	32,84	35,61	28,76	32,86
CH_4 $(\%\ vol.)*$	Experimental	11,4	10	9,4	9,4	10,2
	Dang et al., 2020	11,42	8,08	7,46	9,73	9,99
	Model	14	10,55	9,57	10,73	10,64
RMSE	Dang et al., 2020	1,26	2,76	4,17	1,17	2,16
	Model	1,81	2,89	4,21	2,62	2,16

Table 3.3: Comparison of model results with Dang et al. [11] results and Campoy et al. [11] experimental results, expressed as composition of the non-condensable gaseous phase on a dry N_2-free basis

In general, the model shows a good accuracy, even if the RMSE is a bit greater than Dang model's one.

Once the model has been validated (Case 1), several changes were done, in terms of biomass composition, gasifying agent and reactor geometry.

First of all, a different biomass is considered as feed. Pine 126, taken from Phyllis2 database, is considered, since it has a certain content in terms of N, Cl and S, so the model generates inert contaminants too, which were not considered in Dang's model, since the N, Cl and S content was neglected

in the biomass used (Table 3.2). The proximate and ultimate analysis of the considered biomass are reported in the table below (Table 3.4) [46].

Proximate analysis	%\wt.	Ultimate analysis	%\wt.
Moisture	10,90	Carbon	51,58
Fixed Carbon	14,07	Hydrogen	5,78
Volatile Matter	85,70	Nitrogen	0,06
Ash	0,23	Chlorine	0,02
		Sulfur	0,01
		Oxygen	42,32

Table 3.4: Pine #126 biomass composition [46]

Since the focus of this work is the integration of biomass gasification and high temperature water electrolysis, which supplies as products hydrogen and oxygen - and this one can be used as gasifying agent - a mixture of steam and oxygen is used as gasifying agent in the model.

The gasifying agent ("GASAGEN") is fed to the system at 400°C and ambient pressure.

It was chosen to keep constant the inlet gas superficial velocity (u_0) with respect to the case with air and steam as gasifying agent, so it is necessary to reduce the geometry of the reactor, and in particular the diameters. Having reduced the diameters (D), also the heights (H) are adapted, keeping constant the D/H ratio, both for bed and freeboard (Case 2) (Table 3.5).

		Case 1	Case 2
Wet biomass mass flow	[kg/h]	15	15
Gasifying agent		air + steam	oxygen + steam
Bed diameter	[m]	0.15	0.11
Freeboard diameter	[m]	1.40	1
Bed height	[m]	0.25	0.18
Total height	[m]	3.55	2.5

Table 3.5: Geometrical parameters for the gasifier with steam and air (Case 1) and with steam and oxygen (Case 2) as gasifying agent

3.4 Solid Oxide Electrolytic Cell (SOEC)

As it was done for the external drying section (3.2), the Solid Oxide Cell Unit uses two unit operation blocks to simulate a single piece of equipment, connected with an extra stream that has not a real physical meaning ("IN-SOEC"), as shown in Figure 3.4.

In this modelling approach there is no distinction between anode and cathode of the SOEC: a hot steam stream enters into the system and it stands both for cathode inlet stream and anode inlet stream ("sweep gas").

A mixture of hydrogen, oxygen and steam is produced, which has to be separated in the two product streams by a separator ("SEPSOEC").

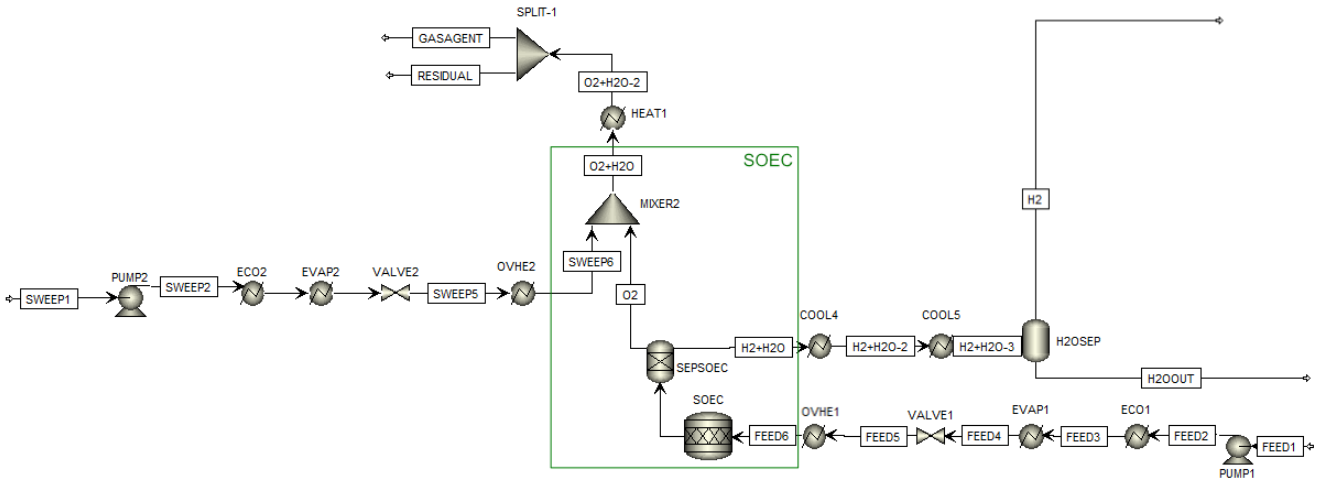

Figure 3.4: SOEC unit flowsheet

The feed stream "FEED1" is liquid water which has to be heated-up to 800°C before being feed to the SOEC, a RStoich block ("SOEC"), which is used to model the electrolysis reaction:

$$2\,H_2O \longrightarrow O_2 + 2\,H_2$$

The RStoich block is used when the stoichiometry and the molar conversion is known for each reaction that takes place. The reaction occurring and a fractional conversion is specified.

The reactor operates at a constant temperature (800°C) and no pressure drops are considered along the reactor.

An intermediate flow (“IN-SOEC”) is used to connect the RStoich to the Separator (“SEPSOEC”), used to divide the product outlet stream into the two product streams: a mixture of H_2 and not-reacted steam, and a stream of pure oxygen.

The pure oxygen is then mixed up with a stream of hot steam (“SWEEP6”), which is in the same conditions of the feed stream when it enters the SOEC (“FEED6”).
This is done to simulate the effect of the sweep gas, which is used to “clean” the anode from the produced oxygen. It is added at the end of the reactor to be sure that it does not participate in the electrolysis reaction.
The mole flow of the input sweep stream ("SWEEP1") is obtained with a calculator block in order to have, at the outlet of the anode, a mixture $O_2 + H_2O$ with the same molar composition of the gasifying agent sent to the gasifier.

The mixture of hydrogen and steam which is obtained at the outlet of the cathode can be treated in order to condense and separate the water. The pure hydrogen stream obtained is sent to the methanation unit, where it is used to enrich the hydrogen content of the raw syngas, which is used as feed for the methanation reactions.

The SOEC is modeled with a Design Specification so that the hydrogen sent to the methanation unit allows to satisfy the stoichiometric parameter requirement for the methanation reactions (which is called “FEED parameter”).

On the other hand the mixture of oxygen and steam, which is obtained at the outlet of the anode, can be used as gasifying agent for the gasification unit. In order to do this, it has to be cooled down until the desired temperature - in this case 400°C - is reached.
Since the SOEC is modeled to fulfill the hydrogen requirement of the system, a part of this mixture will be split (with "SPLIT-1") and it will not be sent to the gasifier ("RESIDUAL").

3.5 Syngas cleaning unit

The syngas cleaning is of great importance and interest, since the raw syngas produced into the gasifier has to meet some “purity” requirements before being used for any downstream application.

In particular, methanation requires high purity and cleanliness, especially from sulphur compounds, which can cause poisoning of the catalysts used in the methanation reactions.

Another big issue is represented by tars, which can condense when temperature is reduced, leading to obstruction and clogging of downstream pipes and equipment.

In this work a simplifying approach was chosen to model syngas cleaning, as represented below in Figure 3.5.

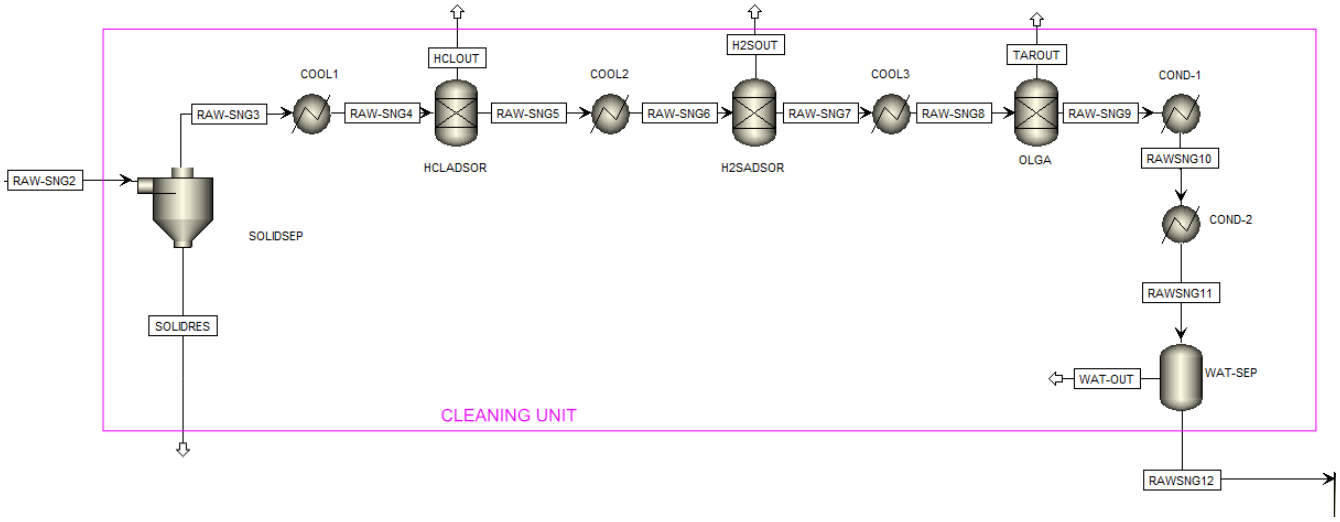

Figure 3.5: Cleaning unit flowsheet

First of all a cyclone ("SOLIDSEP") is used to separate un-reacted char, and in general all the suspended solid particles and dust, from the produced raw syngas coming out from the gasifier. In this model, the un-reacted char is the only solid material considered at the outlet of the gasifier.
All the clean-up systems are modeled with a very simplifying approach, as it was done for the in-bed cleaning step, with a series of separators and coolers, used to reduce the stream temperature to the operating temperatures of the different processes.

HCl and H_2S adsorption is performed at 550°C and 400°C respectively [32]. A more detailed approach for the syngas cleaning is described by Marcantonio et al., modelling the reactions of the sorbents with these two contaminants. In this work it is assumed that HCl and H_2S are completely absorbed and removed from the stream.

NH_3 was almost completely removed with dolomite into the gasifier, with a given separation yield of 95%.

For tars a mid-low temperature system was chosen and modeled again with a simplifying approach with a Separator block. It was assumed almost

a full removal of these species, by imposing a separation yield of the 99%, which can be achieved for example with oil based scrubbers (OLGA system) [30]. The operating temperatures of the OLGA system usually are in the range from 380 to 70°C [47].

After the tars removal stage, the raw syngas is cooled down to 30°C so that almost all the water content is condensed and separated by another Separator block (“WAT-SEP”).

3.6 Methanation unit

The simulation model of the methanation unit is shown in Figure 3.6.

The raw syngas produced in the gasifier, cleaned in the cleaning unit from all its contaminants and separated from water, is enriched by the pure hydrogen stream coming from the SOEC unit ("H_2"), in order to fulfill the stoichiometric requirement for the methanation reactions. This is done in the simulation environment with a mixer block (“MIXER3”).

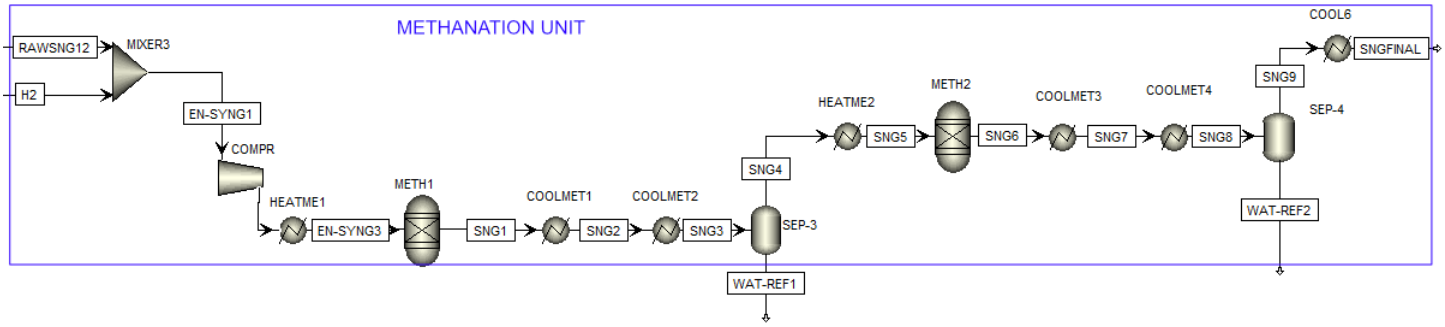

Figure 3.6: Methanation unit flowsheet

The enriched syngas is pressurized up to 16 bars and heated up to 280°C. The RGibbs reactor (“METH1”, “METH2”) was employed to simulate the behavior of a methanation reactor, calculating the chemical and phase equilibrium by minimizing the Gibbs free energy of the system. For this reason, it is not needed to specify the reactions that occur within the methanator. No pressure drops have been considered into the reactor.

To reach very high methane concentrations, up to the 97-98% vol., two cooled methanators with an intermediate condensation stage, in order to remove the produced water, were chosen and modeled.

At the end of the process a stream of almost pure methane (“SNGFINAL”) is obtained. It has to meet some requirements, in terms of composition, heating value, Wobbe’s Index and relative density to be injected into the grid [48]. If these requirements are not met, the syngas has to be further treated and enriched.

Chapter 4

Simulation results and process integration

In this section all the most important results of the model described in Chapter 3 will be discussed.
In particular great attention will be given to the gasification unit results, which is the main difference with respect to the work done by Giglio et al.
Furthermore, the gasification unit could be considered the "core" of the model, since on the basis of the raw syngas composition obtained at the outlet of the gasifier, all the other parts of the plant are dimensioned, in particular the SOEC.

4.1 Sensitivity analysis

First of all a sensitivity analysis was performed, in order to evaluate the effect of some relevant parameters on the gasifier's performances.

A simplified assumption was done in this first part of the results' evaluation: the three parameters, which are Equivalence Ratio (ER), Steam-to-Biomass Ratio (SBR) and gasification temperature ($T_{gas,set}$), were considered as independent one from each other.

As it will be discussed later, gasification temperature is strictly dependent on ER and SBR.
In this part it is assumed that a control system is available, which makes possible to set a desired value of gasification temperature ($T_{gas,set}$).

4.1.1 Effect of ER on syngas composition

Two constant values of gasification temperature (850°C) and SBR (0.35) were set, while ER was varied in the range from 0.2 to 0.35.
The molar composition of the dry non-condensable gaseous phase was evaluated for 10 different values of ER.

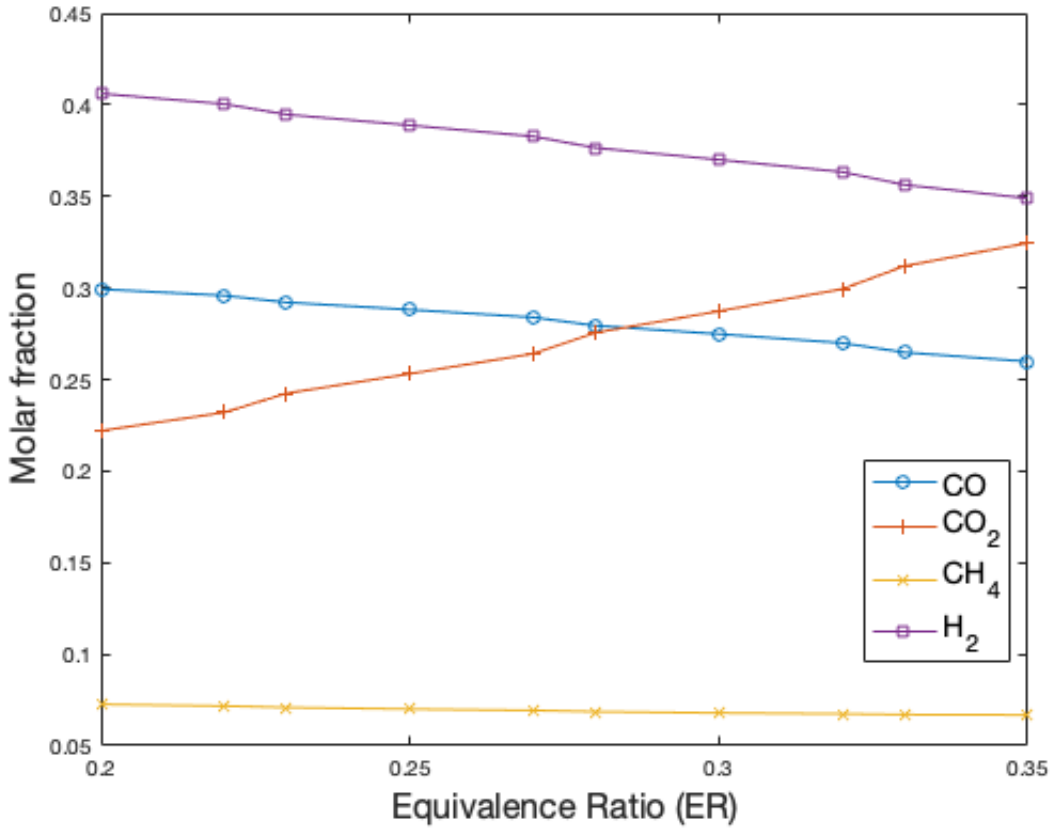

Figure 4.1: Dry syngas molar composition as a function of ER at T = 850°C and SBR = 0.35

When the oxygen content in the gasifying agent is increased, and thus ER, the oxidation reaction of CO and H_2 within the reactor are enhanced, so we can observe from the trends in Figure 4.1 that CO and H_2 concentrations decrease of almost 5%mol, while CO_2 molar concentration increases from 22.2% to 32.5%.
CH_4 concentration is not very affected by the increase of ER and it remains almost constant at around 7%mol.

4.1.2 Effect of SBR on syngas composition

Two constant values of gasification temperature (850°C) and ER (0.27) were set, while SBR was varied in the range from 0.2 to 0.5.
The molar composition of the dry non-condensable gaseous phase was evaluated for 10 different values of SBR.

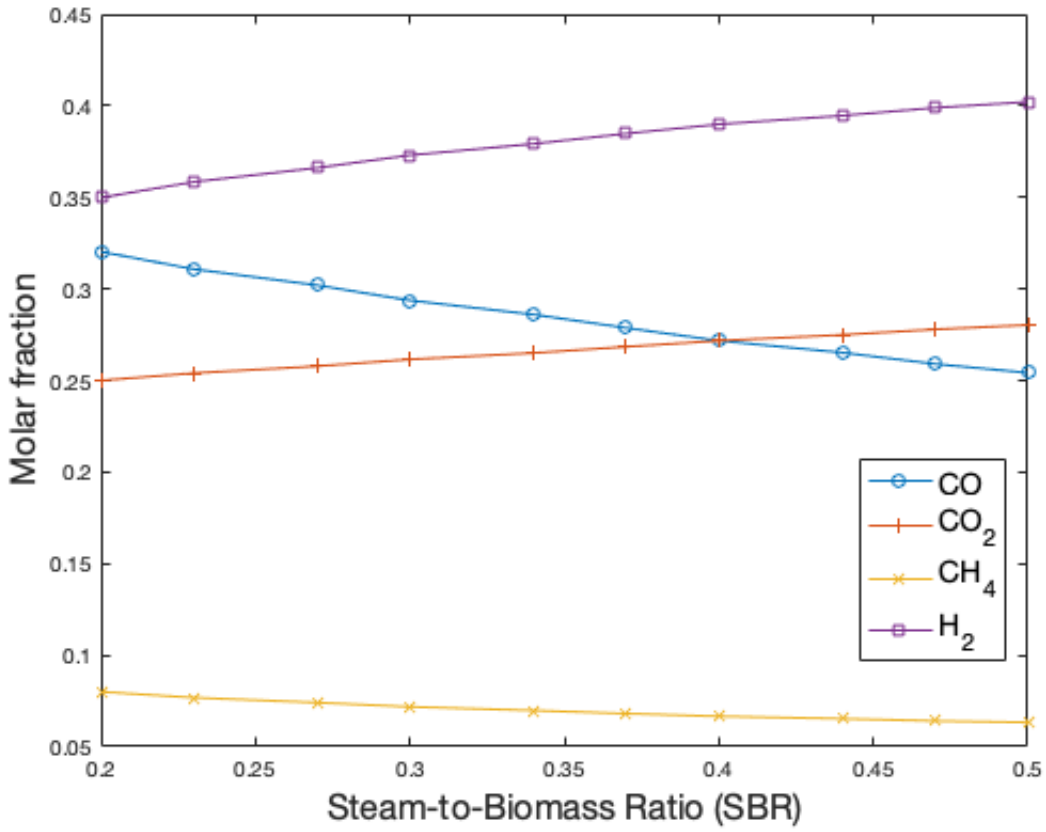

Figure 4.2: Dry syngas molar composition as a function of SBR at T = 850°C and ER = 0.27

H_2 concentration increases, when the steam content in the gasifying agent mixture is increased, thus the SBR. This happens because, with higher H_2O concentrations, the reactions of steam gasification of the char, Steam Methane Reforming (SMR) and Water Gas Shift (WGS) are favoured, leading to a boost in the production of H_2.

For the same reason, CO_2 concentration increases, as it is a product of the WGS reaction. On the other hand, since CO is a reactant for the WGS, its concentration is reduced when SBR is increased.

As it happened when ER was varied keeping constant $T_{gas,set}$ and SBR, methane concentration is affected only slightly by the variation of SBR in the considered range and it remains almost constant, since SMR reaction is slower than WGS.

4.1.3 Effect of temperature on syngas composition

The gasification temperature was varied in the range 750-1100°C, with an incremental step of 50°C. ER and SBR were kept constant at 0.27 and 0.35 respectively.
The molar fractions of the single non-condensable gaseous species when temperature is varied are shown in Figure 4.3.

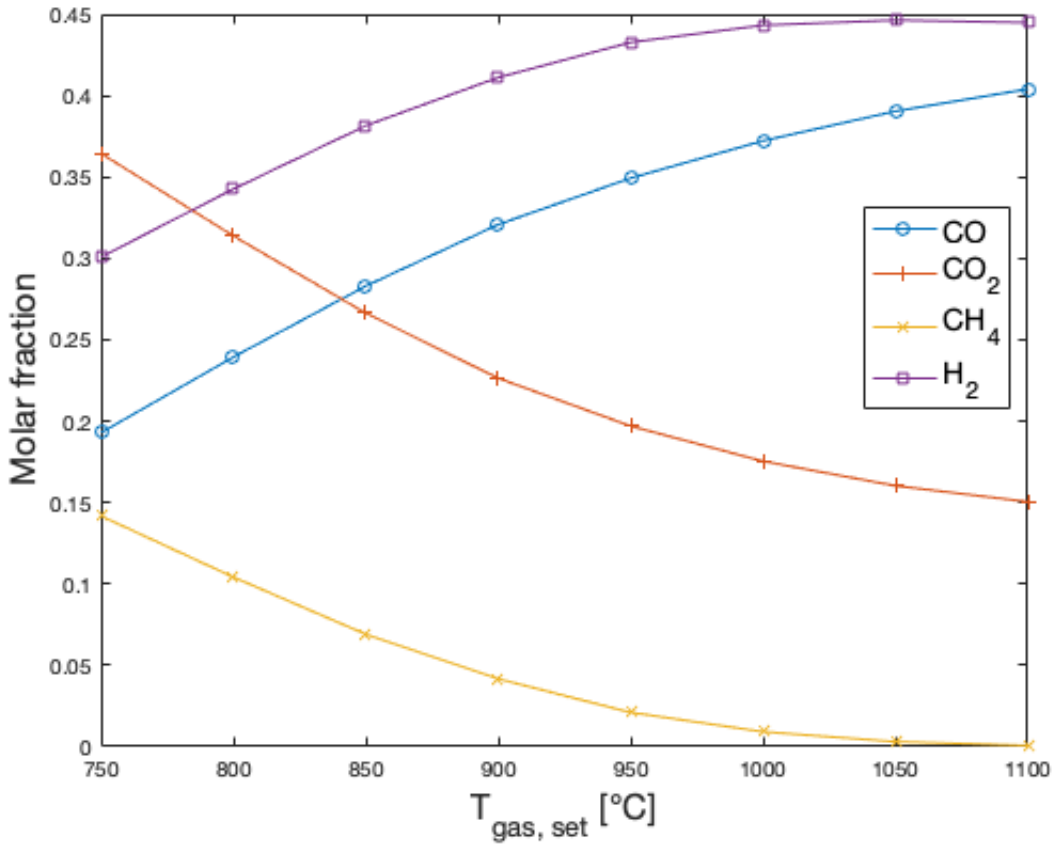

Figure 4.3: Dry syngas molar composition as a function of T_{gas} with ER = 0.27 and SBR = 0.35

At relatively low temperatures (750-850°C) a consistent fraction of CH_4 is

produced (15-10%vol.). This content is significantly reduced when the temperature increases and it becomes nearly 0% when high values of temperature are reached (1050°C or more). This because the higher the temperature, the higher the reaction rate of the SMR, thus the methane consumption.

For the same reason CO and H_2 content increases with increasing temperature, because the SMR is favoured at high temperatures. Also, high temperatures provide the required energy for the endothermic char gasification reactions, and in particular the steam gasification one.

Furthermore, at high temperatures, the Reverse Water Gas Shift (RWGS) reaction is favoured, leading, both with the enhancement of the Boudouard reaction (CO_2 gasification reaction), to a decrease in CO_2 concentration with increasing temperature.

4.2 Parameters dependency

In the previous section the effect of every single parameter (ER, SBR, $T_{gas,set}$) was evaluated on the syngas molar composition.

Now the gasification temperature T_{gas} is not considered anymore as a set value, but it is the temperature which makes the gasifier working in adiabatic conditions. Under this assumption, the gasification temperature is not considered anymore as an independent variable.

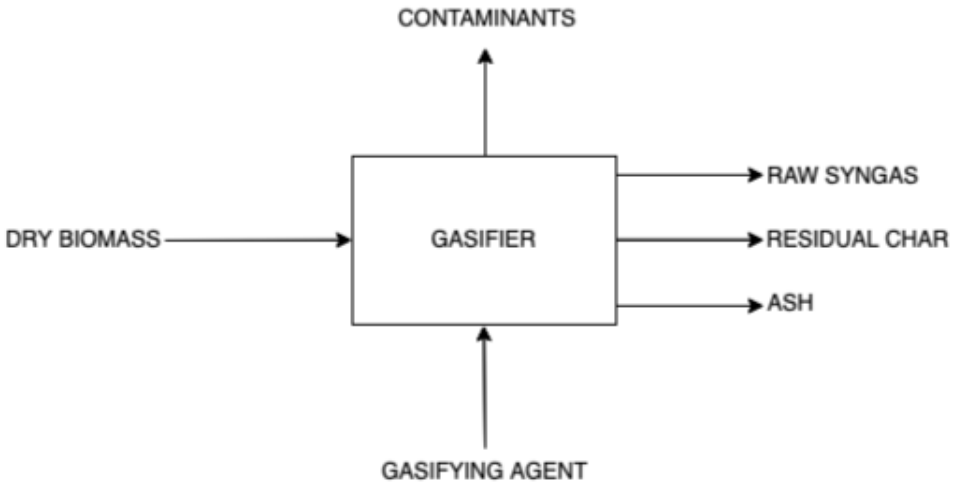

Figure 4.4: Gasifier control volume

In other words, it is the temperature which ensures to have

$$\dot{m}_{biom} \cdot h_{biom} + \dot{m}_{gas,agen} \cdot h_{gas,agen} + \dot{m}_{char} \cdot h_{char} + \dot{m}_{ash} \cdot h_{ash} + \dot{m}_{syng} \cdot h_{syng} = 0$$

Actually also heat losses from gasifier walls should be taken into account. In this case they are neglected.

The gasification temperature is evaluated for different values of ER and SBR, which are shown in the next sections.

4.2.1 Effect of ER on T_{gas}

In order to determine the effect of ER on the gasification temperature, the value of SBR was fixed at 0.35 and a sensitivity analysis was performed varying the ER value, thus the gasifying oxygen mass flow, in a range from 0.20 to 0.35.

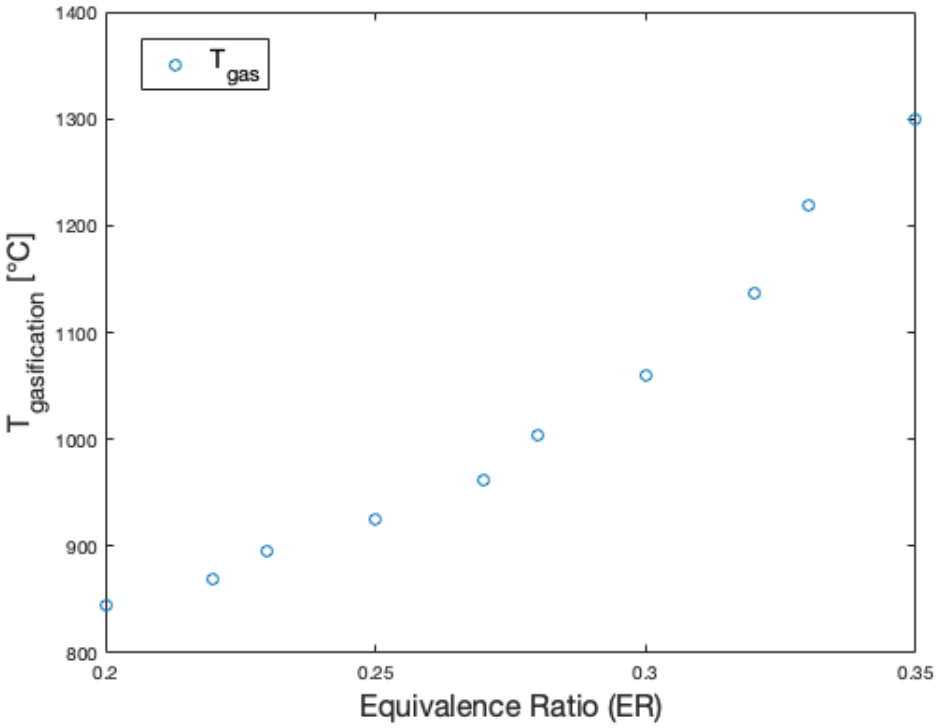

Figure 4.5: T_{gas} as a function of ER

As the ER is increased, T_{gas} increases too. This happens mainly because the oxidation reactions are favoured due to higher oxygen concentrations.

An increment of almost 500°C is observed by varying the ER in the range from 0.2 to 0.35, keeping SBR constant at 0.35.

4.2.2 Effect of ER on syngas molar composition

To observe the effect of ER on the syngas molar composition, first of all the value of SBR is set at 0.35.

When the ER is changed, the T_{gas} changes too, as it was shown in 4.2.1, so the molar composition will be affected at the same time by a change in ER and in temperature.

This means that in Figure 4.6 a different gasification temperature is associated to each ER value.

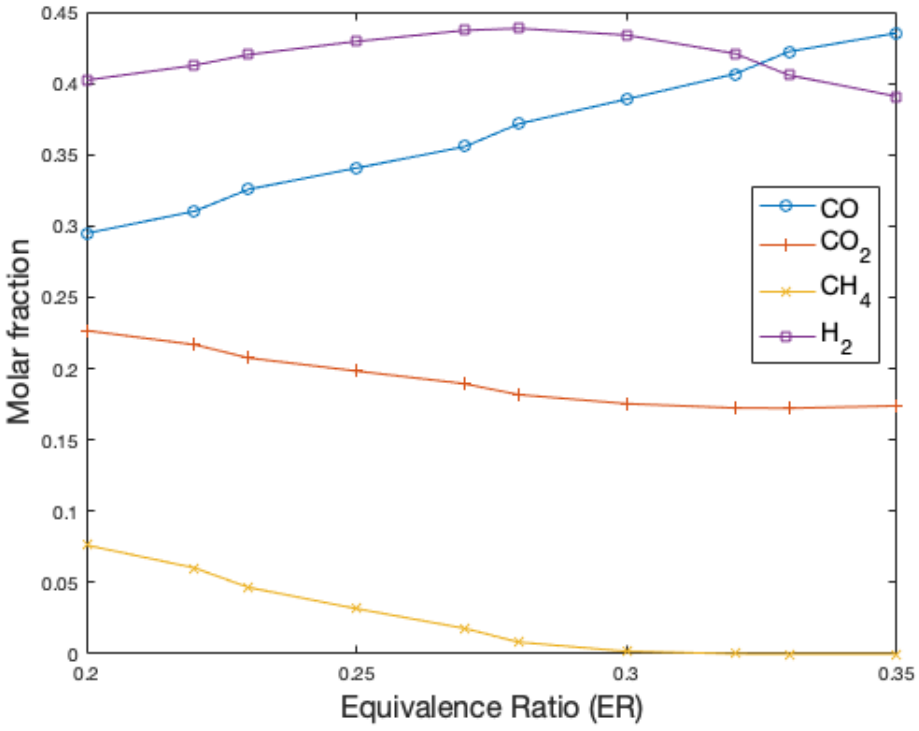

Figure 4.6: Molar composition of the syngas as a function of ER and T_{gas}

H_2 shows a particular trend: its yield increases with increasing ER (and temperature), it reaches a maximum at around ER = 0.27 and then it starts to decrease. For values of ER lower than this threshold, the effect of the increasing gasification temperature prevails and the molar concentration of the

hydrogen tends to increase (4.1.3). After this value the oxidation reactions take over and the hydrogen molar concentration slowly decreases, since the hydrogen is oxidized faster (4.1.1).

For CO and CO_2 the temperature has an higher impact than the ER, so both species follow the trends shown in Figure 4.3, even if with a smaller slope.

CH_4 tends to decrease and its concentration is nearly 0% for high values of ER and T_{gas}.

4.2.3 Effect of SBR on T_{gas}

In order to determine the effect of SBR on the gasification temperature, the value of ER was fixed at 0.27 and a sensitivity analysis was performed varying the SBR value, thus the gasifying steam mass flow, in a range from 0.20 to 0.50.

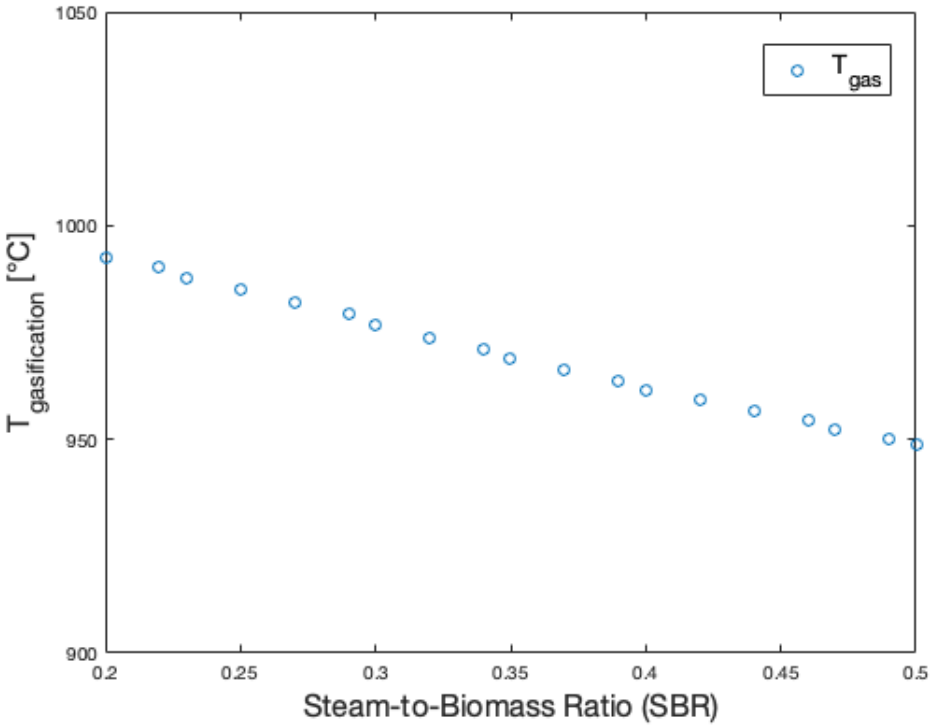

Figure 4.7: T_{gas} as a function of SBR

As the SBR is increased, T_{gas} has a slight decrease. This happens mainly

because the endothermic reduction reactions are favoured, due to an increase in concentration of steam.

With respect to the ER, it has a smaller impact, since the gasification temperature is reduced only about 50°C varying SBR in the range from 0.2 to 0.5.

4.2.4 Effect of SBR on syngas molar composition

First of all it is chosen a fixed value of ER, equal to 0.27. The SBR was varied in the range from 0.2 to 0.5.

When SBR is changed, the gasification temperature changes too, as it was shown in 4.2.3. This means that each point represented in Figure 4.7 corresponds to a different value of SBR and T_{gas}, with T_{gas} decreasing when SBR is increased.

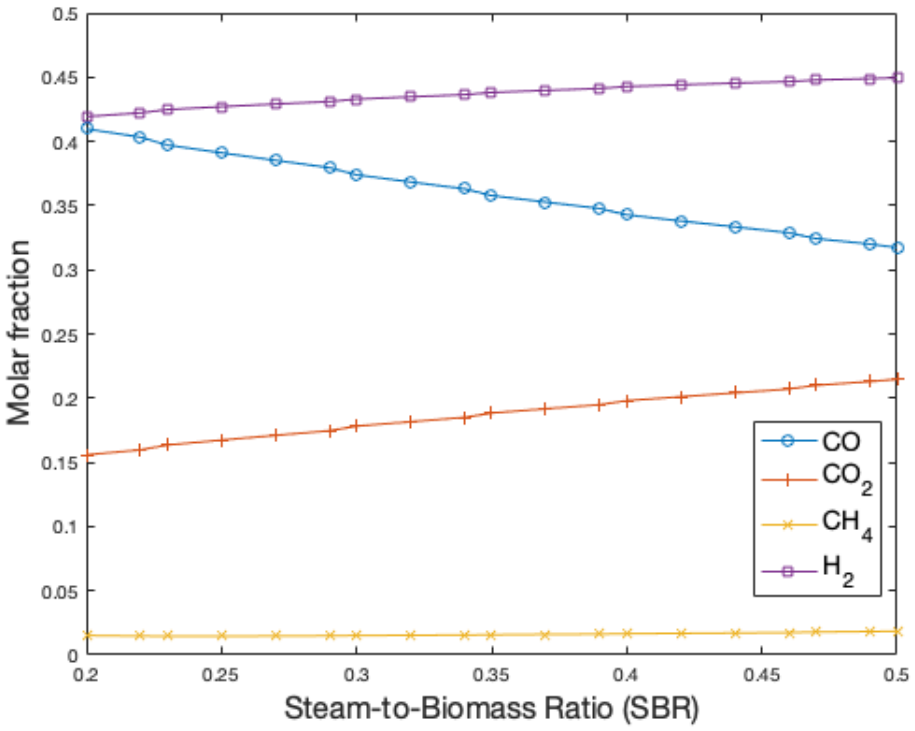

Figure 4.8: Molar composition of the syngas for different values of ER and T_{gas}

In general the SBR has an higher impact on the molar composition of the raw syngas, with respect to temperature.

H_2 concentration increases because the gasifying steam content increases and thus the reactions leading to H_2 formation, even if the temperature is slightly reduced by the increase of SBR at fixed values of ER.

CO and CO_2 tend to decrease and increase respectively, due to the combined effect of temperature decrease and SBR increase.

For CH_4 concentrations, the effect of SBR and temperature is balanced, so it tends to remain almost constant when the conditions are varied.

4.3 System optimization

The parameter chosen to optimize the system is the feed gas module ($FEED$), which represents the stoichiometric requirement for both the methanation reactions, which should be equal to 3.

$$FEED = \frac{y_{H_2} - y_{CO_2}}{y_{CO} + y_{CO_2}}$$

It was evaluated for different values of ER and SBR (and so of T_{gas}), in order to find the values of these parameters which maximize it.

A parametric analysis was performed.
10 different values of SBR in the range 0.20-0.50 were chosen and, for each of them, the gasification temperature, the molar composition of the dry non-condensable gaseous phase and the FEED parameter were evaluated for 10 different values of ER in the range 0.20-0.35.
In Table 4.1 only 3 chosen values of SBR are reported, as an example to show the trend of the considered parameters.

As previously written, the gasification temperature increases with increasing ER and slightly decreases with increasing SBR (Figure 4.9).

But the most important parameter to be evaluated in this section is the Feed Gas Module.

Of course it follows the hydrogen trend, being proportional to it: it increases with the increase of ER, until it reaches a maximum at around ER = 0.28 and then it starts to decrease again. Even if the H_2 production increases with increasing SBR, the FEED parameter shows lower local maximum for higher values of SBR. This happens because, at the same time, the CO_2 production increases, thus having an impact on the numerator of the FEED expression (Figure 4.10).

			MOLAR COMPOSITION				
SBR	ER	T_{gas} [°C]	CO	CO_2	CH_4	H_2	FEED
0.20	0.20	859.09	0.3404	0.1989	0.0781	0.3826	0.3406
	0.22	883.78	0.3564	0.1892	0.0639	0.3905	0.3691
	0.23	913.60	0.3703	0.1795	0.0454	0.4049	0.4099
	0.25	945.84	0.3844	0.1703	0.0292	0.4160	0.4429
	0.27	982.30	0.3992	0.1619	0.0166	0.4223	0.4641
	0.28	1027.28	0.4150	0.1544	0.0070	0.4236	0.4729
	0.30	1094.95	0.4326	0.1488	0.0010	0.4177	0.4625
	0.32	1186.01	0.4497	0.1471	1.52E-05	0.4033	0.4293
	0.33	1277.47	0.4644	0.1475	2.24E-08	0.3880	0.3930
	0.35	1368.90	0.4774	0.1495	1.13E-12	0.3731	0.3566
0.35	0.20	843.96	0.2948	0.2267	0.0763	0.4022	0.3366
	0.22	869.84	0.3104	0.2168	0.0603	0.4125	0.3713
	0.23	895.70	0.3258	0.2075	0.0466	0.4201	0.3987
	0.25	925.77	0.3406	0.1983	0.0317	0.4294	0.4290
	0.27	961.52	0.3556	0.1894	0.0179	0.4371	0.4544
	0.28	1003.17	0.3716	0.1817	0.0082	0.4385	0.4643
	0.30	1060.21	0.3889	0.1754	0.0018	0.4338	0.4578
	0.32	1136.52	0.4066	0.1724	8.62E-05	0.4209	0.4292
	0.33	1219.70	0.4222	0.1722	5.44E-07	0.4057	0.3929
	0.35	1303.02	0.4358	0.1736	2.80E-10	0.3906	0.3560
0.50	0.20	830.59	0.2543	0.2524	0.0770	0.4162	0.3232
	0.22	855.91	0.2695	0.2429	0.0613	0.4264	0.3582
	0.23	881.99	0.2844	0.2337	0.0467	0.4353	0.3892
	0.25	909.17	0.2993	0.2249	0.0339	0.4419	0.4139
	0.27	940.93	0.3142	0.2164	0.0213	0.4481	0.4366
	0.28	979.70	0.3298	0.2085	0.0104	0.4513	0.4510
	0.30	1026.25	0.3462	0.2020	0.0037	0.4481	0.4488
	0.32	1090.67	0.3636	0.1944	4.13E-04	0.4380	0.4274
	0.33	1164.59	0.3796	0.1886	9.31E-06	0.4234	0.3925
	0.35	1239.48	0.3937	0.1848	3.84E-08	0.4084	0.3559

Table 4.1: Evaluation of the molar composition of the syngas and FEED parameter as a function of ER for different values of SBR

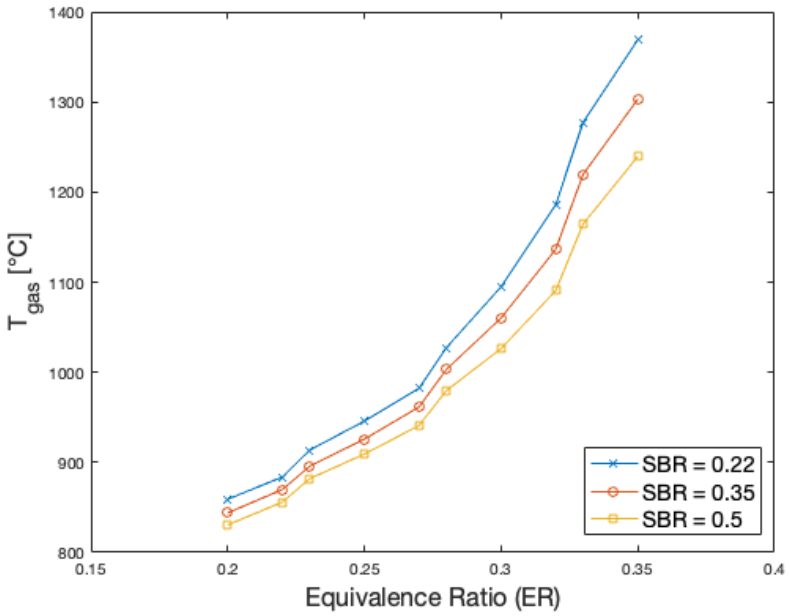

Figure 4.9: Gasification temperature as a function of ER for different values of SBR

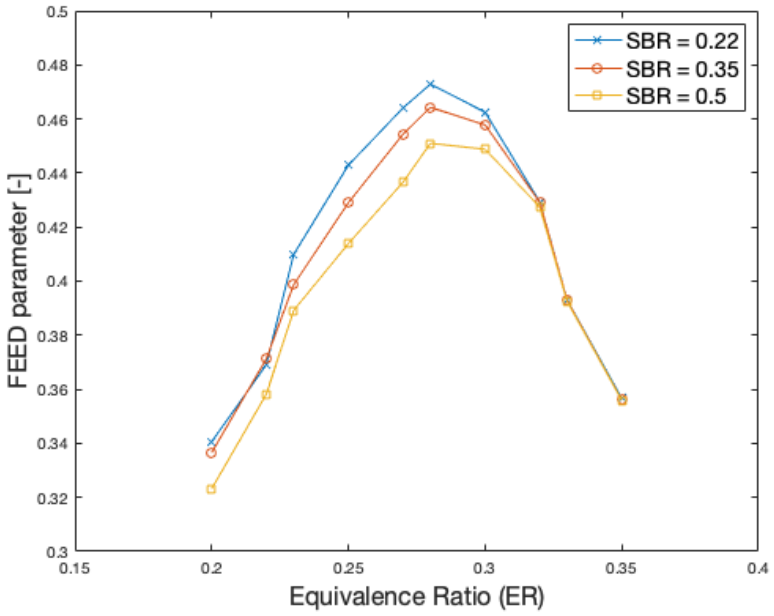

Figure 4.10: FEED parameter as a function of ER for different values of SBR

After this first analysis, 10 different values of ER in the range 0.20-0.50

were chosen and for each of them the gasification temperature, the molar composition of the non-condensable gaseous phase and the FEED parameter were evaluated for 10 different values of SBR in the range 0.20-0.50.

In Table 4.2 only 3 chosen values of ER are reported, as an example to show the trend of the considered parameters.

As previously written, the gasification temperature slightly decreases with increasing SBR and increases with increasing ER (Figure 4.11).

Also in this case, the parameter of greatest interest in this section is the Feed Gas Module.

Even if the hydrogen concentration increases with increasing SBR, the FEED parameter tends to decrease or to remain almost constant for higher values of ER, since the carbon dioxide concentration rises too, for the effect of the increasing SBR and decreasing temperature. Also in this case it is possible to notice the impact of the ER that was discussed previously, with FEED increasing until a maximum is reached at around ER = 0.28 and then decreasing again (Figure 4.12).

After this analysis, it is possible to determine an "optimal" operating point, in terms of ER and SBR, which maximizes the FEED parameter of the outlet syngas stream, thus the relative molar concentration of hydrogen in the mixture.

The ER should be high enough to ensure a suitable gasification temperature in order to enhance Steam Methane Reforming reaction and the endothermic char gasification reactions. At the same time, it has to be contained within a certain value in order to don’t enhance the oxidation reactions which would lead to a consumption of the hydrogen.

The operating point is set then to ER = 0.281 and SBR = 0.20, resulting in a gasification temperature of 1031°C and a Feed Gas Module of the outlet syngas of 0.4740.

			MOLAR COMPOSITION				
ER	SBR	T_{gas} [°C]	CO	CO_2	CH_4	H_2	FEED
0.20	0.20	861.69	0.3483	0.1942	0.0788	0.3786	0.3398
	0.23	857.19	0.3347	0.2023	0.0777	0.3853	0.3408
	0.27	852.96	0.3220	0.2100	0.0770	0.3911	0.3404
	0.30	849.02	0.3102	0.2172	0.0765	0.3961	0.3392
	0.34	845.36	0.2991	0.2241	0.0763	0.4006	0.3374
	0.37	841.94	0.2887	0.2306	0.0762	0.4046	0.3351
	0.40	838.72	0.2789	0.2367	0.0763	0.4081	0.3325
	0.44	835.68	0.2696	0.2426	0.0765	0.4113	0.3295
	0.47	832.81	0.2610	0.2481	0.0767	0.4142	0.3261
	0.50	830.59	0.2543	0.2524	0.0770	0.4162	0.3232
0.27	0.20	989.00	0.4080	0.1567	0.0159	0.4194	0.4653
	0.23	983.77	0.3954	0.1644	0.0156	0.4246	0.4647
	0.27	978.05	0.3835	0.1719	0.0158	0.4288	0.4626
	0.30	972.55	0.3722	0.1790	0.0161	0.4326	0.4600
	0.34	967.33	0.3614	0.1859	0.0166	0.4361	0.4572
	0.37	962.36	0.3510	0.1925	0.0171	0.4394	0.4541
	0.40	957.61	0.3412	0.1989	0.0176	0.4423	0.4508
	0.44	953.04	0.3317	0.2050	0.0182	0.4450	0.4471
	0.47	948.55	0.3227	0.2109	0.0190	0.4474	0.4431
	0.50	944.66	0.3157	0.2156	0.0199	0.4488	0.4389
0.35	0.20	1380.39	0.4839	0.1458	3.34E-13	0.3703	0.3565
	0.23	1361.53	0.4724	0.1525	1.71E-12	0.3751	0.3563
	0.27	1343.38	0.4613	0.1589	8.58E-12	0.3798	0.3561
	0.30	1325.81	0.4505	0.1651	4.27E-11	0.3844	0.3562
	0.34	1309.39	0.4400	0.1712	1.66E-10	0.3888	0.3561
	0.37	1294.05	0.4297	0.1772	5.23E-10	0.3931	0.3558
	0.40	1278.59	0.4198	0.1828	1.98E-09	0.3973	0.3559
	0.44	1264.48	0.4102	0.1884	5.49E-09	0.4014	0.3558
	0.47	1250.25	0.4009	0.1937	1.74E-08	0.4053	0.3559
	0.50	1239.48	0.3937	0.1979	3.84E-08	0.4084	0.3559

Table 4.2: Evaluation of the molar composition of the syngas and FEED parameter as a function of SBR for different values of ER.

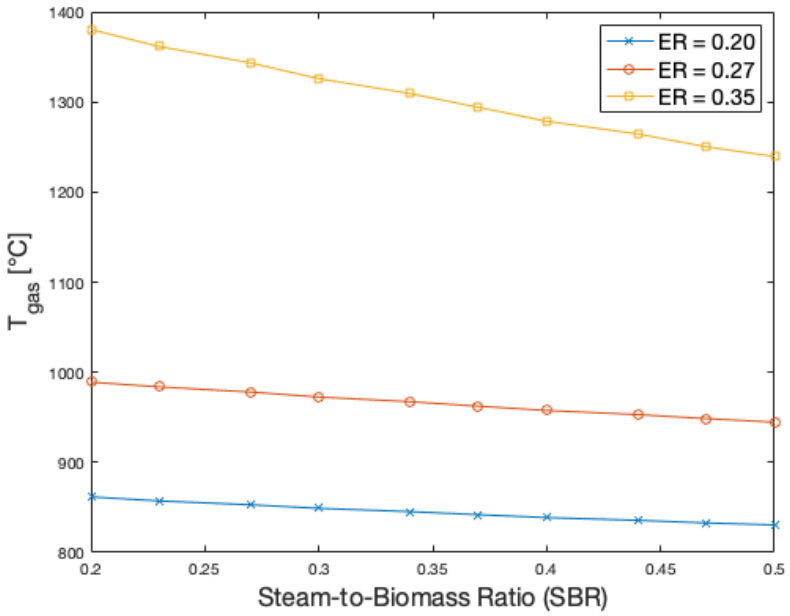

Figure 4.11: Gasification temperature as a function of SBR for different values of ER

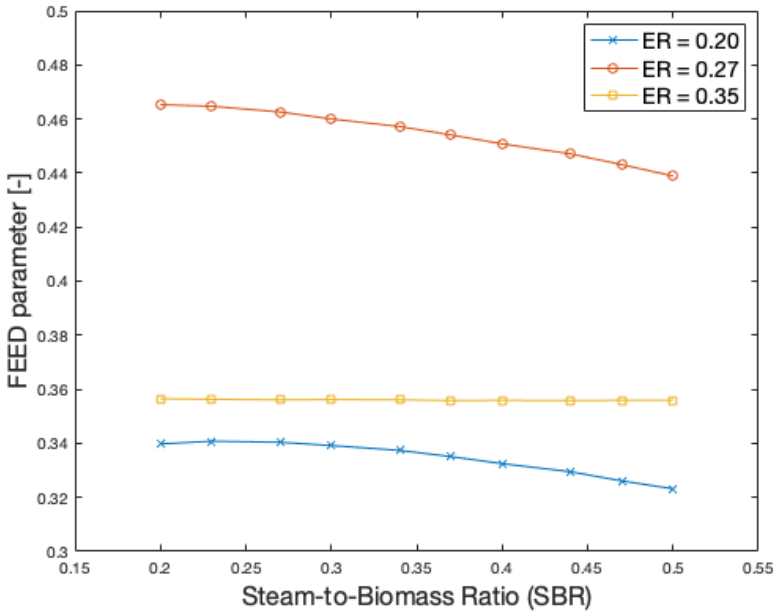

Figure 4.12: FEED parameter as a function of ER for different values of SBR

4.4 Tar production estimation

One of the most important improvements of this model with respect to the equilibrium one is that it is possible to model tars production and it is possible to evaluate its trend when the operating conditions are varied.

Actually, an assumptions which over-estimates tar production was done. It is assumed that, during the devolatilization stage, the tar yield is equal to 5% on a dry biomass basis. This assumption does not take in consideration a temperature dependency for the tar yield: in other words, the tar yield will be always equal to the same value, even if the devolatilization temperature is varied.

Another limit of the model is that only few tar cracking reactions were found in literature (R9, R10, R11 and R12 in Table 3.1).

100 simulation runs were performed, varying ER in the range 0.20-0.35 and SBR in the range 0.20-0.50, in order to evaluate the model behavior in terms of tar production. Some of these test results are reported in the following sections.

Two parameters were considered in the evaluation of the tar content at the outlet of the gasifier:

- Tar yield, expressed in terms of g of tars over kg of dry biomass;
- Tar concentration, expressed in terms of g of tars over Nm^3 of dry raw syngas.

4.4.1 Effect of ER on tar yield and concentration

As it was previously discussed, when ER and SBR are changed, gasification temperature changes too. In particular, when ER is increased, temperature increases too, since the oxidation reactions are favoured.

As it is shown in Table 4.3, as ER increases, the tar yield increases too. This might seem strange, but as it is shown in Table 4.4, the overall tar produced in terms of molar flow decreases when ER - thus T_{gas} - is increased.

On the other hand, at the outlet of the devolatilization stage, only two species were considered to characterize tars ($C_3H_6O_2$ and C_7H_8). Now three other species are considered and, with C_6H_6O and C_7H_8 being heavier in terms of molecular weight, as a result we see an increase in the tar yield.

The tar concentration (Figure 4.13) decreases and then it increases again with increasing ER. This happens because the dry raw syngas volumetric flow first increases (as shown in 4.2.2 and in Figure 4.6, this is the same trend of the hydrogen molar fraction as a function of ER), until a certain value of ER

is reached (≈ 0.28). After this value, the oxidation reactions are enhanced, more water is produced, and the dry raw syngas volumetric flow is reduced again.

SBR [-]	ER [-]	T_{gas} [°C]	$\dot{V}_{syng}$ [Nm^3/h]	$\dot{m}_{tar}$ [kg/h]	Tar yield [$g_{tar}/kg_{dry,biom}$]	x_{tar} [$g/Nm^3_{dry,syng}$]
0.20	0.20	861.73	19.168	0.6611	48.971	34.490
	0.23	917.21	20.110	0.6627	49.086	32.952
	0.27	985.57	20.817	0.6638	49.171	31.889
	0.30	1101.17	20.755	0.6647	49.236	32.025
	0.33	1287.84	19.753	0.6654	49.287	33.685
0.33	0.20	845.69	19.817	0.6258	46.357	31.580
	0.23	897.62	20.756	0.6306	46.709	30.380
	0.27	963.97	21.360	0.6353	47.062	29.744
	0.30	1064.83	21.337	0.6398	47.390	29.983
	0.33	1226.58	20.361	0.6438	47.690	31.620
0.50	0.20	830.59	20.372	0.5790	42.891	28.423
	0.23	882.00	21.242	0.5892	43.641	27.735
	0.27	940.93	21.904	0.5958	44.130	27.199
	0.30	1026.25	21.979	0.6003	44.469	27.313
	0.33	1164.59	21.047	0.6037	44.719	28.684

Table 4.3: Tar yield and concentration as a function of ER for different values of SBR

SBR [-]	ER [-]	$\dot{n}_{tar}$ [kmol/s]	$C_3H_6O_2$ [$\%mol$]	C_7H_8 [$\%mol$]	C_6H_6O [$\%mol$]	$C_{10}H_8$ [$\%mol$]	C_6H_6 [$\%mol$]
0.20	0.20	2.26187E-06	55.31349	38.41085	0.00061	0.05071	6.22434
	0.23	2.25918E-06	55.22061	28.15905	0.00073	0.09038	16.52924
	0.27	2.25371E-06	55.03093	8.93274	0.00088	0.17145	35.86400
	0.30	2.23558E-06	54.39584	0.00179	0.00157	0.44267	45.15183
	0.33	2.16248E-06	51.80399	≈ 0	0.00547	1.50406	46.68648
0.33	0.20	2.26274E-06	55.34373	40.61235	0.00058	0.03779	4.00555
	0.23	2.26082E-06	55.27729	33.78289	0.00068	0.06616	10.87298
	0.27	2.25669E-06	55.13439	16.75282	0.00083	0.12721	27.98475
	0.30	2.24483E-06	54.72112	0.23592	0.00108	0.30388	44.73801
	0.33	2.20047E-06	53.14407	≈ 0	0.00349	0.97186	45.88058
0.50	0.20	2.26341E-06	55.36668	42.09436	0.00055	0.02799	2.51042
	0.23	2.26191E-06	55.31517	37.42795	0.00065	0.04997	7.20626
	0.27	2.25913E-06	55.21898	25.51381	0.00078	0.09105	19.17539
	0.30	2.25191E-06	54.96820	3.72736	0.00098	0.19823	41.10523
	0.33	2.22631E-06	54.06752	≈ 0	0.00209	0.58245	45.34694

Table 4.4: Tar molar composition as a function of SBR for different values of ER

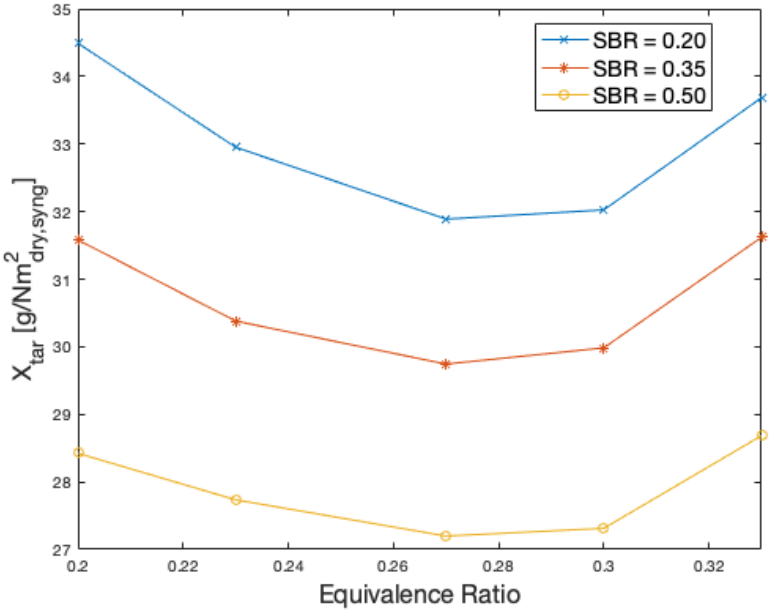

Figure 4.13: Tar concentration as a function of ER for different values of SBR.

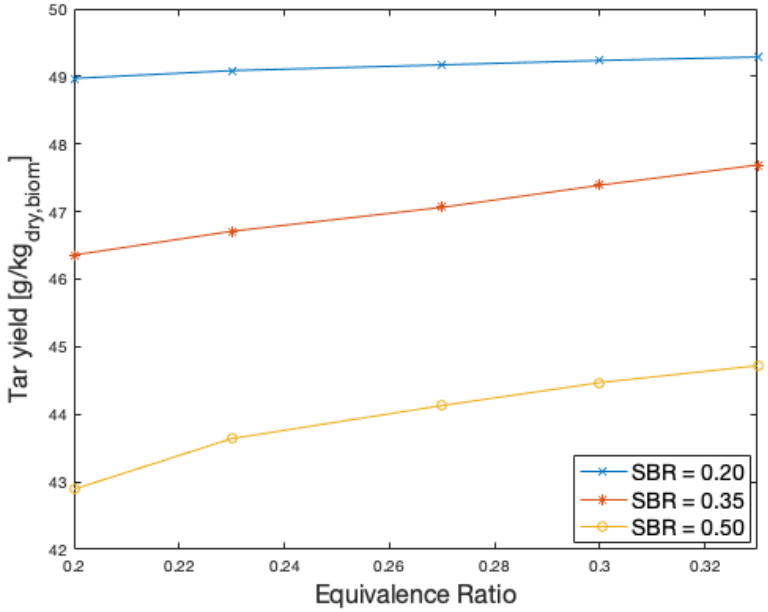

Figure 4.14: Tar yield as a function of ER for different values of SBR.

At higher temperatures, the molar composition of the tars is shifted more towards the heavier products, so the tar yield increases.

Also it has to be considered that the cracking reaction of C_6H_6 is not considered, so its content tends only to increase even at very high temperatures.

4.4.2 Effect of SBR on tar yield and concentration

Now the SBR is varied at different values of ER. When SBR increases, the gasification temperature decreases.

As it is shown in Table 4.5, as SBR increases, tar yield and tar concentration tend to decrease.

Also in this case, it might seem a strange behavior. This happens for two reasons mainly:

- first of all, the volumetric flow of dry raw syngas increases, since H_2 and CO_2 content increases with higher SBR, as it was shown in 4.2.4 (Figure 4.8);
- secondly, as it is shown in Table 4.6, with increasing SBR - thus lower T_{gas} - the initial tar species are less converted into the other components. This means that at the outlet of the gasifier there will be an higher tar molar flow, but with lighter weight, resulting in a lower mass flow rate.

In other words, at higher SBR and lower temperatures, the tar molar flow has an higher relative content of "light" species, so at the outlet of the gasifier there will be a lower mass flow rate of tars with respect to the the cases with higher temperatures. This means that there will be a lower concentration and tar yield, as highlighted in the figures below (Figure 4.15, Figure 4.16).

To know more about the tar conversion within the system, the tar molar flow should be the most considered parameter in this specific case, at least until the model is not improved with other reactions which could characterize the behavior of the heavier species too.

In general, the higher the temperature, the lower the tar content in the outlet stream from the gasifier.

ER [-]	SBR [-]	T_{gas} [°C]	$\dot{V}_{syng}$ [Nm^3/h]	$\dot{m}_{tar}$ [kg/h]	Tar yield [$g_{tar}/kg_{dry,biom}$]	x_{tar} [$g/Nm^2_{dry,syng}$]
0.20	0.20	861.73	19.168	0.6611	48.971	34.490
	0.27	853.17	19.517	0.6488	48.063	33.245
	0.33	845.69	19.817	0.6258	46.357	31.580
	0.40	839.14	20.070	0.6120	45.335	30.494
	0.43	836.14	20.181	0.6066	44.931	30.057
	0.50	830.59	20.372	0.5790	42.891	28.423
0.27	0.20	985.57	20.817	0.6638	49.171	31.889
	0.27	974.37	21.101	0.6556	48.563	31.069
	0.33	963.97	21.360	0.6353	47.062	29.744
	0.40	954.55	21.587	0.6142	45.493	28.450
	0.43	950.10	21.692	0.6106	45.227	28.147
	0.50	940.93	21.904	0.5958	44.130	27.199
0.35	0.20	1380.57	19.300	0.6657	49.308	34.489
	0.27	1344.16	19.584	0.6600	48.889	33.701
	0.33	1310.88	19.864	0.6458	47.839	32.511
	0.40	1280.58	20.135	0.6195	45.892	30.769
	0.43	1266.67	20.263	0.6135	45.445	30.277
	0.50	1239.48	20.527	0.6051	44.822	29.475

Table 4.5: Tar mass flow and yield as a function of SBR for different values of ER

ER [-]	SBR [-]	$\dot{n}_{tar}$ [kmol/s]	$C_3H_6O_2$ [$\%mol$]	C_7H_8 [$\%mol$]	C_6H_6O [$\%mol$]	$C_{10}H_8$ [$\%mol$]	C_6H_6 [$\%mol$]
0.20	0.20	2.26187E-06	55.31349	38.41085	0.00061	0.05071	6.22434
	0.27	2.26236E-06	55.33044	39.67291	0.00059	0.04347	4.95259
	0.33	2.26274E-06	55.34373	40.61235	0.00058	0.03779	4.00555
	0.40	2.26305E-06	55.35431	41.32038	0.00056	0.03327	3.29147
	0.43	2.26318E-06	55.35883	41.61044	0.00056	0.03134	2.99882
	0.50	2.26341E-06	55.36668	42.09436	0.00055	0.02799	2.51042
0.27	0.20	2.25371E-06	55.03093	8.93274	0.00088	0.17145	35.86400
	0.27	2.25535E-06	55.08700	12.80576	0.00086	0.14710	31.95841
	0.33	2.25669E-06	55.13439	16.75282	0.00083	0.12721	27.98475
	0.40	2.25778E-06	55.17208	20.44165	0.00081	0.11110	24.27436
	0.43	2.25825E-06	55.18845	22.16378	0.00080	0.10410	22.54287
	0.50	2.25913E-06	55.21898	25.51381	0.00078	0.09105	19.17539
0.35	0.20	2.08771E-06	49.58297	≈0	0.00881	2.04948	48.35867
	0.27	2.12832E-06	50.71505	≈0	0.00711	1.84195	47.43589
	0.33	2.15722E-06	51.63649	≈0	0.00573	1.55726	46.80051
	0.40	2.17843E-06	52.36428	≈0	0.00465	1.28637	46.34470
	0.43	2.18685E-06	52.66086	≈0	0.00421	1.16867	46.16626
	0.50	2.20142E-06	53.17947	≈0	0.00344	0.95640	45.86069

Table 4.6: Tar molar composition as a function of SBR for different values of ER

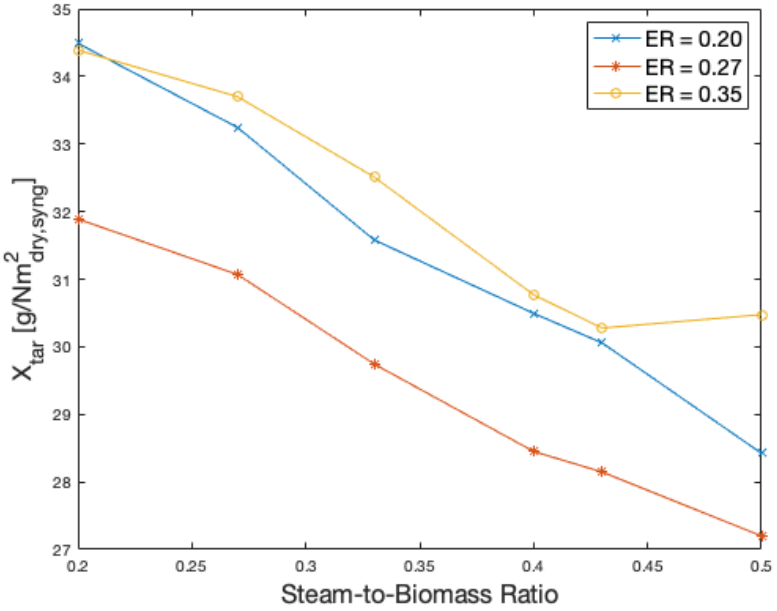

Figure 4.15: Tar concentration as a function of SBR for different values of ER.

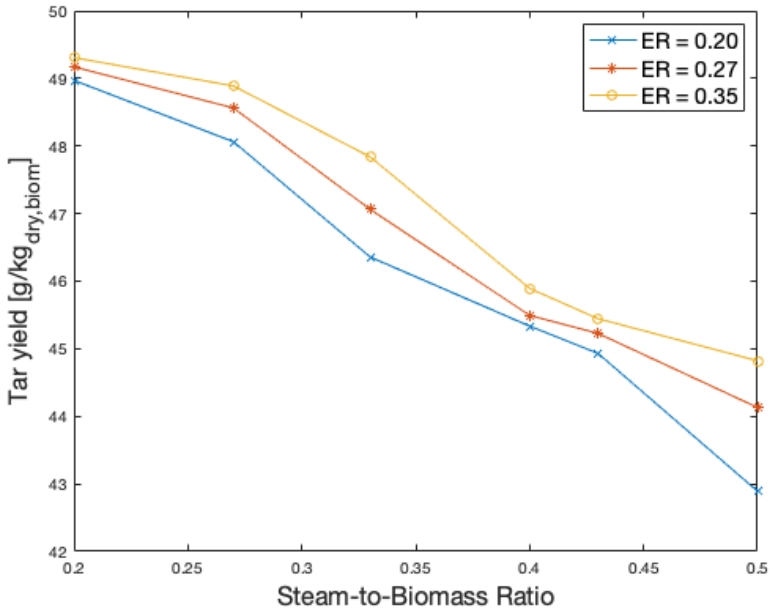

Figure 4.16: Tar yield as a function of SBR for different values of ER.

4.5 Electrolysis integration

Having defined an optimal operating point, it is now possible to dimension the SOEC Unit.
It has to produce the hydrogen needed to enrich the raw syngas exiting the gasifier, to make it fulfill the Feed Module Gas before it is sent to the methanation unit.
This is done on ASPEN Plus by mean of a Design Specification.

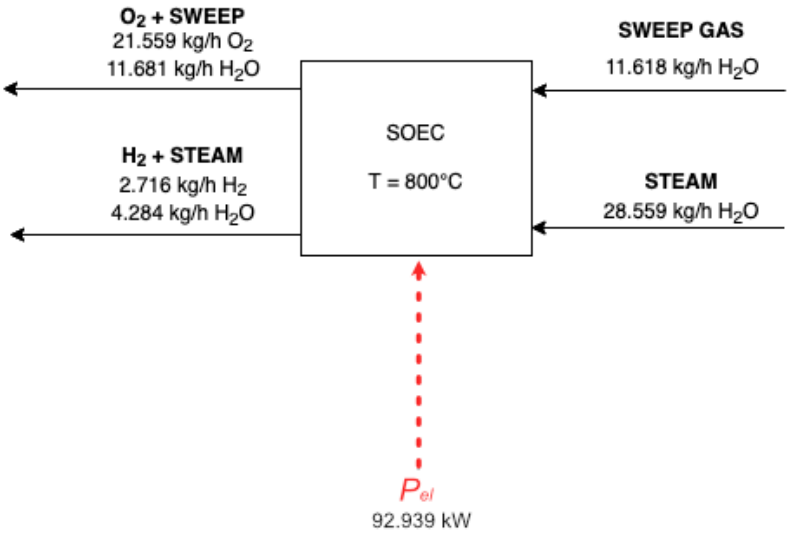

Figure 4.17: Control volume of the electrolysis unit in the optimal configuration

In the considered operating conditions, 28.559 kg/h of steam are sent to the SOEC as feed. At the outlet there will be:

- cathode side 2.716 kg/h of hydrogen and 4.284 kg/h of non-reacted steam, which will be separated in order to obtain a stream of pure hydrogen to enrich the raw syngas hydrogen content up to the desired value;
- anode side 21.559 kg/h of oxygen and 11.681 kg/h of sweep steam. In

this way, the same molar composition of the gasifying agent is obtained, thus part of the stream can be sent to the gasifier.

An electrical energy input is required to do this, and it is equal to 92.929 kW, since the SOEC is assumed to work near thermoneutral conditions.

4.6 Methanation performances

The methanation unit has the aim to obtain a gas stream which has at least 97% molar of CH_4.

In order to do this, in this work two methanation stage were considered, with an intermediate cooling stage used to remove the produced water within the first reactor.

The molar compositions at the inlet and at the outlet of each methanation stage are highlighted in Table 4.7, considering as reference for the stream names Figure 3.6.

		EN-SYNG3	SNG3	SNG5	SNG8	SNGFINAL
MASS FLOW	[KG/H]	22.27525	22.27525	8.910118	8.910118	8.700862
CO	[$\%mol.$]	16.67	<1	<1	<1	<1
CO_2	[$\%mol.$]	5.92	0.46	1.07	0.17	0.17
CH_4	[$\%mol.$]	0.27	40.85	94.45	97.12	99.20
H_2	[$\%mol.$]	73.66	1.82	4.20	0.58	0.59
H_2O	[$\%mol.$]	3.48	56.87	0.28	2.13	0.04
Other	[$\%mol.$]	<1	<1	<1	<1	<1

Table 4.7: Methanation unit streams molar compositions

4.7 Possible thermal integration

The methanation process is a highly exothermic process. For this reason, the operating methanation temperature has to be controlled and a cooling system is necessary.

On the other hand, the plant has some important energy input requirements, for example for the evaporation of the liquid water used as feed for the SOEC and as sweep gas to "clean" the anode outlet.

The heat produced in the methanators - which are two in this case ("METH1" and "METH2") - can be then supplied as evaporation heat to the evaporators ("EVA1" and "EVA2" for SOEC feed steam and sweep gas respectively, Figure

3.6).

Component name	Heat [kW]
METH1	-30.2487
METH2	-0.2153
EVAP1	+14.1030
EVAP2	+5.7681

Table 4.8: Heat produced or required in the optimal system configuration

In Table 4.3, the "-" sign is used for produced heat, hence for an exothermic process; "+" is used for required heat, then for an endothermic process.

Chapter 5

Conclusions

A process configuration for the production of synthetic natural gas (SNG) starting from woody biomass was proposed and analyzed. The whole process was modeled and analyzed using ASPEN Plus process simulator integrated with an external FORTRAN subroutine to represent properly the gasification of biomass in a bubbling fluidized bed (BFB) gasifier in terms of hydrodynamics and reaction kinetics.

The gasification stage performances, in terms of outlet stream composition, were analyzed by varying some operating parameters like equivalence ratio (ER) and steam-to-biomass ratio (SBR), thus the gasification temperature.

Proper values of ER and SBR were set to maximize hydrogen content within the produced syngas. This operating point was found to be at ER = 0.281 and SBR = 0.20, resulting in a gasification temperature of 1031°C and a Feed Gas Module of the outlet syngas of 0.4740.

A solid oxide electrolysis cell (SOEC) system for water splitting was modeled then on the basis of the results obtained in the gasification unit: hydrogen produced at cathode side, in fact, is mixed with the syngas exiting the gasifier unit, to reach the stoichiometric syngas composition for the subsequent methanation reaction, where carbon monoxide and carbon dioxide are hydrogenated in a catalytic reactor to produce synthetic methane (FEED = 3).

In the considered gasifier operating conditions, 28.559 kg/h of steam are sent to the SOEC as feed cathode side. At the outlet, cathode side, 2.716 kg/h of hydrogen mixed with 4.284 kg/h of non-reacted steam are obtained. The steam is separated with a condensation stage and the pure hydrogen stream is sent to the methanation unit.

Part of the oxygen-steam mixture from anode outlet, on the other hand, is exploited as gasifying agent into the biomass gasification unit. 21.559 kg/h of oxygen and 11.681 kg/h of sweep steam are obtained at the outlet anode side. A part (5.408 kg/h and 2.93 kg/h of oxygen and steam respectively) is sent to the gasifier. The other part of the mixture can be stored or used for other purposes.

An electrical energy input is required to do this, and it is equal to 92.929 kW, since the SOEC is assumed to work near thermoneutral conditions.

In Figure 5.1 all the main results are highlighted, in terms of required energy input, mass flow rates and operating temperatures. The "Contaminants" stream exiting from the Clean-up Units block is a mixture of water, HCl, NH_3, H_2S and tars.

It has to be noticed that in the H_2 stream, used to enrich the cleaned syngas which is sent to the gasifier, a small amount of water in vapour phase is entrained, and that's the reason why the mass flow rate is higher than the pure hydrogen one.

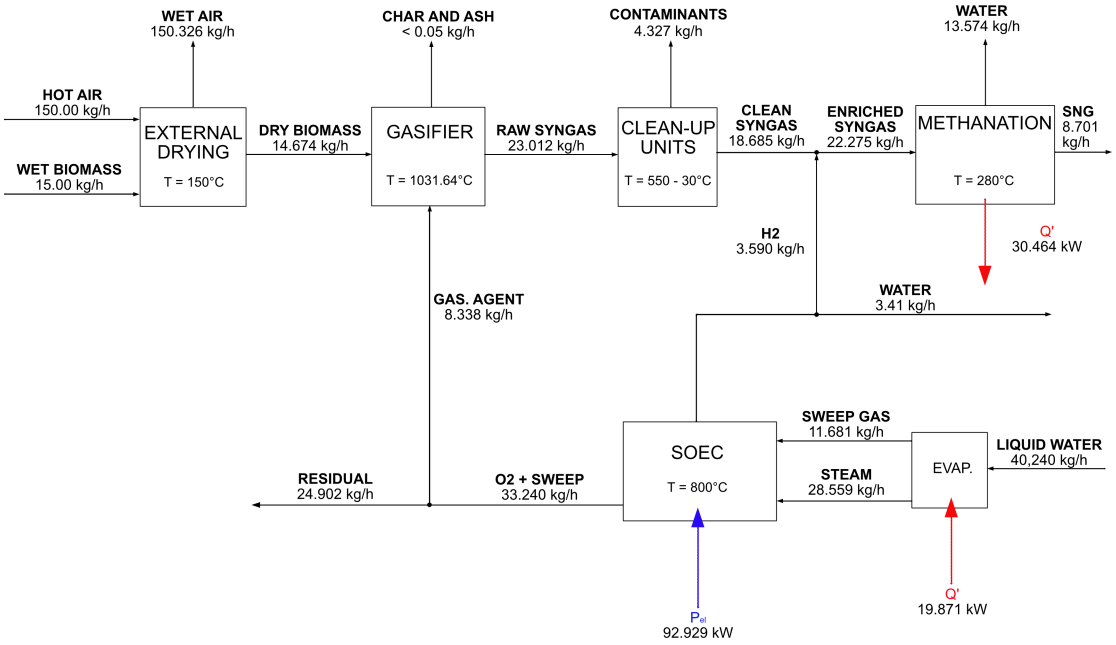

Figure 5.1: Simplified flowchart with main model results

5.1 Recommendations for future works

The following recommendations are suggested to make some refinements to the model:

- Validation of the model on other and different experimental data sets;
- The use of a kinetic approach for the other parts of the plant, to obtain results which would be closer to reality;
- More detailed representation of the syngas clean-up unit: in this work a very simplified approach was considered. All the syngas clean up stages were represented with a separator block on ASPEN Plus. A more complete model should take into account all the physical and chemical processes needed for the cleaning of the syngas. Furthermore, in this work complete - or almost complete - removal of contaminants like Cl, N, S compounds and tars was considered. Actually in the produced SNG part of these contaminants could still be present and their concentration should be evaluated to determine if the produced gas could be injected into the grid;
- Improvements could be done on the hydrodynamics and on the reaction kinetics considering more detailed equations and more gasification reactions;
- A different approach for the tar content evaluation could be useful: in this work, it is assumed that, during the devolatilization stage, tar yield is 5%wt. on a dry basis at every temperature. This assumption overestimates the tar production, which is actually reduced at higher temperatures. The implementation of a temperature-dependant approach could be interesting in this sense, also to have a more accurate prediction of the outlet syngas composition in terms of tars;
- A thermal integration within the different units and stages of the plant can be performed, as mentioned in Section 4.7 "Possible thermal integration".

Bibliography

[1] IEA. (2020) World energy balances: Overview. [Online]. Available: https://iea.blob.core.windows.net/assets/23f096ab-5872-4eb0-91c4-418625c2c9d7/World_Energy_Balances_Overview_2020_edition.pdf

[2] P. McKendry, "Energy production from biomass (part 1): Overview of biomass," *Bioresource Technology*, vol. 83(1), pp. 37–46, May 2002, doi: 10.1016/s0960-8524(01)00118-3.

[3] A. A. Ahmad, N. A. Zawawi, F. H. Kasim, A. Inayat, and A. Khasri, "Assessing the gasification performance of biomass: A review on biomass gasification process conditions, optimization and economic evaluation," *Renewable and Sustainable Energy Reviews, Elsevier*, vol. 53(C), pp. 1333–1347, 2016, doi: 10.1016/j.rser.2015.09.030.

[4] F. Berruti, "Biomass gasification," 26 Novembre - 4 Dicembre 2014, politecnico di Torino.

[5] M. A. Mac Kinnon and S. S. Brouwer, J, "The role of natural gas and its infrastructure in mitigating greenhouse gas emissions, improving regional air quality, and renewable resource integration," *Process in Energy and Combustion Science*, vol. 64(C), 2018, doi: doi:10.1016/j.pecs.2017.10.002.

[6] M. Pozzo, A. Lanzini, and M. Santarelli, "Enhanced biomass-to-liquid (btl) conversion process through high temperature co-electrolysis in a solid oxide electrolysis cell (soec)," *Fuel*, vol. 145, pp. 39–49, 2015, doi: https://doi.org/10.1016/j.fuel.2014.12.066.

[7] Q. Bernical, X. Joulia, I. Noirot-Le Borgne, P. Floquet, P. Baurens, and G. Boissonnet, "Sustainability assessment of an integrated high temperature steam electrolysis-enhanced biomass to liquid fuel process," *Ind. Eng. Chem. Res.*, vol. 52, no. 22, pp. 7189–7195, 2013, doi: dx.doi.org/10.1021/ie302490y.

[8] L. Clausen, N. Houbak, and B. Elmegaard, "Technoeconomic analysis of a methanol plant based on gasification of biomass and electrolysis of water," *Energy*, vol. 35, no. 55, pp. 2338–2347, 2010, doi:

10.1016/j.energy.2010.02.034.

[9] E. Giglio, G. Vitale, A. Lanzini, and M. Santarelli, “Integration between biomass gasification and high-temperature electrolysis for synthetic methane production,” *Biomass and Bioenergy*, vol. 148, no. 106017, 2021, doi: https://doi.org/10.1016/j.biombioe.2021.106017.

[10] M. Campoy, A. Gómez-Barea, A. L. Villanueva, and P. Ollero, “Air-steam gasification of biomass in a fluidized bed under simulated autothermal and adiabatic conditions,” *Ind. Eng. Chem. Res.*, vol. 47, pp. 5957–5965, 2008, doi: 10.1021/ie800220t.

[11] Q. Dang, X. Zhang, Y. Zhou, and X. Jia, “Prediction and optimization of syngas production from a kinetic-based biomass gasification process model,” *Fuel Processing Technology*, no. 106604, 2020, doi: https://doi.org/10.1016/j.fuproc.2020.106604.

[12] O. Schmidt, I. Gambhir, I. Staffel, A. Hawkes, J. Nelson, and S. Few, “Future cost and performance of water electrolysis: An expert elicitation study,” *ScienceDirect*, 2017, doi: https://doi.org/10.1016/j.ijhydene.2017.10.045.

[13] UNFCCC. Annex 8 - clarifications on definition of biomass and consideration of changes in carbon polls due to a cdm project activity. [Online]. Available: https://cdm.unfccc.int/Reference/Guidclarif/mclbiocarbon.pdf

[14] G. Huber, S. Iborra, and A. Corma, “Synthesis of transportation fuels from biomass: Chemistry, catalysts and engineering,” *Chem. Rev.*, vol. 106, pp. 4044–4098, 2006, doi: 10.1021/cr068360d.

[15] J. Watson, Y. Zhang, B. Si, W.-T. Chen, and R. de Souza, “Gasification of biowaste: A critical review and outlooks,” *Renewable and Sustainable Energy Reviews*, vol. 83, pp. 1–17, 2018, doi: https://doi.org/10.1016/j.rser.2017.10.003.

[16] P. Basu, *Biomass Gasification, Pyrolysis and Torrefaction*. Academic Press, Elsevier, 2013.

[17] G. Haarlemmer, “Simulation study of improved biomass drying efficiency for biomass gasification plants by integration of water gas shift section in the drying process,” *Biomass and Bioenergy*, vol. 81, pp. 129–136, 2015, doi: http://dx.doi.org/10.1016/j.biombioe.2015.06.002.

[18] K. Holmgren, T. Berntsson, E. Andersson, and T. Rydberg, “System aspects of biomass gasification with methanol synthesis - process concepts and energy analysis,” *Energy*, vol. 45, pp. 817–828, 2012, doi: http://dx.doi.org/10.1016/j.energy.2012.07.009.

[19] A. Molino, S. Chianese, and D. Musmarra, “Biomass gasification technology: The state of the art overview,” *Journal of Energy Chemistry*, vol. 25,

pp. 10–25, 2016, doi: http://dx.doi.org/10.1016/j.jechem.2015.11.005.

[20] Q. Miao, J. Zhu, S. Barghi, C. Wu, X. Yin, and Z. Zhou, “Modeling biomass gasification in circulating fluidized beds,” *Renewable Energy*, vol. 50, pp. 655–661, 2012, doi: http://dx.doi.org/10.1016/j.renene.2012.08.020.

[21] T. Milne, R. Evans, and N. Abatzoglou, “Biomass gasifier "tars": Their nature, formation and conversion,” National Renewable Energy Laboratory, Tech. Rep., 1998.

[22] S. Sansaniwal, K. Pal, M. Rosen, and S. Tyagi, “Recent advances in the development of biomass gasification technology: A comprehensive review,” *Renewable and Sustainable Energy Reviews*, vol. 72, pp. 363–384, 2017, doi: http://dx.doi.org/10.1016/j.rser.2017.01.038.

[23] J. Phillips. Different types of gasifiers and their integration with gas turbines. [Online]. Available: https://netl.doe.gov/sites/default/files/netl-file/1-2-1.pdf

[24] M. La Villetta, M. Costa, and N. Massarotti, “Modelling approaches to biomass gasification: A review with emphasis on the stoichiometric method,” *Renewable and Sustainable Energy Reviews*, vol. 74, pp. 71–88, 2017.

[25] J. Kiel, S. van Paasen, J. Neeft, L. Devi, K. Ptasinski, F. Janssen, R. Meijer, R. Berends, H. Temmink, G. Brem, N. Padban, and E. Bramer. Primary measures to reduce tar formation in fluidised-bed biomass gasifiers. [Online]. Available: https://pure.tue.nl/ws/portalfiles/portal/4367413/576697.pdf

[26] M. Laguna-Bercero, “Recent advances in high temperature electrolysis using solid oxide fuel cells: A review,” *Journal of Power Sources*, vol. 203, pp. 4–16, 2012.

[27] A. Buttler and H. Spliethoff, “Current status of water electrolysis for energy storage, grid balancing and sector coupling via power-to-gas and power-to-liquids: A review,” *Renewable and Sustainable Energy Review*, vol. 82, pp. 2440–2454, 2018.

[28] E. Giglio, A. Lanzini, M. Santarelli, and P. Leone, “Synthetic natural gas via integrated high-temperature electrolysis and methanation: Part i—energy performance,” *Journal of Energy Storage*, vol. 1, pp. 22–37, 2015.

[29] L. Barelli, G. Bidini, and G. Cinti, “Steam as sweep gas in soe oxygen electrode,” *Journal of Energy Storage*, vol. 20, pp. 190–195, 2018.

[30] N. Abdoulmoumine, S. Adhikari, A. Kulkarni, and S. Chattanathan, “A review on biomass gasification syngas cleanup,” *Applied Energy*, vol. 155, pp. 294–307, 2015, doi: http://dx.doi.org/10.1016/j.apenergy.2015.05.095.

[31] Y. Richardson, J. Blin, and A. Julbe, "A short overview on purification and conditioning of syngas produced by biomass gasification: Catalytic strategies, process intensification and new concepts," *Progress in Energy and Combustion Science*, vol. 38, pp. 765–781, 2012.

[32] V. Marcantonio, E. Bocci, J. Ouweltjes, L. Del Zotto, and D. Monarca, "Evaluation of sorbents for high temperature removal of tars, hydrogen sulphide, hydrogen chloride and ammonia from biomass-derived syngas by using aspen plus," *International Journal of Hydrogen Energy*, 2019, doi: https://doi.org/10.1016/j.ijhydene.2019.12.142.

[33] S. Roensch, J. Schneider, S. Matthischke, M. Sclueter, M. Goetz, J. Lefebvre, P. Prabhakaran, and S. Bajohr, "Review on methanation – from fundamentals to current projects," *Fuel*, vol. 166, pp. 276–296, 2016, doi: http://dx.doi.org/10.1016/j.fuel.2015.10.111.

[34] M. Goetz, J. Lefebvre, F. Moers, A. McDaniel Koch, F. Graf, S. Bajohr, R. Reimert, and T. Kolb, "Renewable power-to-gas: A technological and economic review," *Renewable Energy*, vol. 85, pp. 1371–1390, 2016, doi: http://dx.doi.org/10.1016/j.renene.2015.07.066.

[35] AspenTechnologyInc, "Aspen plus® aspen plus user guide version 10.2."

[36] ——, "Aspen plus® getting started modeling processes with solids v8.4."

[37] ——, "Aspen plus® user models v7.0."

[38] M. Nikoo and N. Mahinpey, "Simulation of biomass gasification in fluidized bed reactor using aspen plus," *Biomass and Bioenergy*, vol. 32, pp. 1245–1254, 2008, doi: 10.1016/j.biombioe.2008.02.020.

[39] J. Pauls, N. Mahinpey, and E. Mostafavi, "Simulation of air-steam gasification of woody biomass in a bubbling fluidized bed using aspen plus: A comprehensive model including pyrolysis, hydrodynamics and tar production," *Biomass and Bioenergy*, vol. 95, pp. 157–166, 2016, doi: http://dx.doi.org/10.1016/j.biombioe.2016.10.002.

[40] P. Kaushal, J. Abedi, and N. Mahinpey, "A comprehensive mathematical model for biomass gasification in a bubbling fluidized bed reactor," *Fuel*, vol. 89, pp. 3650–3661, 2010, doi: 10.1016/j.fuel.2010.07.036.

[41] P. Kaushal and R. Tyagi, "Advanced simulation of biomass gasification in a fluidized bed reactor using aspen plus," *Renewable Energy*, vol. 101, pp. 629–636, 2017, doi: http://dx.doi.org/10.1016/j.renene.2016.09.011.

[42] A. Gómez-Barea and B. Leckner, "Estimation of gas composition and char conversion in a fluidized bed biomass gasifier," *Fuel*, vol. 107, pp. 419–431, 2013, doi: http://dx.doi.org/10.1016/j.fuel.2012.09.084.

[43] D. Kunii and O. Levenspiel, "Fluidized reactor models. 1. for bubbling beds of fine, intermediate and large particles. 2. for the lean phase:

Freeboard and fast fluidization," *Ind. Eng. Chem. Res.*, vol. 29, pp. 1226–1234, 1990, doi: https://doi.org/10.1021/ie00103a022.

[44] ——, *Fluidization Engineering. Second Edition.* Butterworth-Heinemann, Elsevier, 1991, doi: https://doi.org/10.1016/C2009-0-24190-0.

[45] S. Mori and C. Wen, "Estimation of bubble diameter in gaseous fluidized beds," *AIChE Journal*, vol. 21, no. 1, pp. 109–115, 1975, doi: https://doi.org/10.1002/aic.690210114.

[46] H. Feldmann, M. Paisley, H. Appelbaum, and D. Taylor, "Conversion of forest residues to a methane-rich gas in a high-throughput gasifier," Battelle Columbus Division for the Pacific Northwest Laboratory, Tech. Rep., 1988.

[47] J.-W. Koenemann and R. Zwart. Olga tar removal technology, paper for power-gen international 2007 in new orleans. - via https://phyllis.nl/Browse/Standard/ECN-Phyllispine%20(126). [Online]. Available: http://b-dig.iie.org.mx/BibDig2/P08-0514/Power_Gen/7c6.pdf

[48] SNAM. Codice di rete di infrastrutture trasporto gas - revisione v. [Online]. Available: https://www.snam.it/export/sites/snam-rp/repository-srg/file/en/business-services/network-code-tariffs/Network_Code_ITG/Archivio_codice_rete/ITG_Codice_di_rete_xvers_Vx_ITA.pdf